Sediment routing systems to the Atlantic rifted margin of the Guiana Shield

Delphine Rouby, Artiom Loparev, Dominique Chardon, Flora Bajolet, Massimo Dall'asta, Fabien Paquet, Charlotte Fillon, Jean-Yves Roig, Jing Ye

Research Paper

GEOSPHERE

GEOSPHERE, v. 19, no. 3

https://doi.org/10.1130/GES02561.1

11 figures; 1 set of supplemental files

CORRESPONDENCE: Delphine.Rouby@get.omp.eu

CITATION: Rouby, D., Loparev, A., Chardon, D., Bajolet, F., Dall'Asta, M., Paquet, F., Fillon, C., Roig, J.-Y., and Ye, J., 2023, Sediment routing systems to the Atlantic rifted margin of the Guiana Shield: Geosphere, v. 19, no. 3, p. 957–974, https://doi.org/10.1130/GES02561.1.

Science Editor: David E. Fastovsky
Associate Editor: Gregory D. Hoke

Received 14 June 2022
Revision received 16 December 2022
Accepted 23 February 2023

Published online 28 April 2023

Sediment routing systems to the Atlantic rifted margin of the Guiana Shield

Delphine Rouby[1], Artiom Loparev[1], Dominique Chardon[1], Flora Bajolet[1,2], Massimo Dall'Asta[3], Fabien Paquet[2], Charlotte Fillon[3], Jean-Yves Roig[2], and Jing Ye[1,3,4]

[1]Géosciences Environnement Toulouse (GET), Université de Toulouse, CNRS, IRD, UPS, CNES, F31400 Toulouse, France
[2]Bureau de Recherches Géologiques et Minières (BRGM), 3 avenue Claude-Guillemin, BP 36009, 45060 Orléans Cédex 02, France
[3]Centre Scientifique et Technique Jean Féger, TOTAL Energies, Avenue Larribau, 64018 Pau Cédex, France
[4]Ali I. Al-Naimi Petroleum Engineering Research Center, King Abdullah University of Science and Technology, Thuwal 23955-6900, Saudi Arabia

ABSTRACT

Sediment routing systems of cratonic domains have not been studied extensively because their relief and erosion rates are very low, although their vast dimensions allowed them to contribute to a significant proportion of the sediments exported to the global ocean. To gain further insights into the behavior of cratonic sediment routing systems at geological time scales, we investigated the Guiana Shield and its Atlantic rifted margin (i.e., the Guiana-Suriname and Foz do Amazonas Basins, northern South America) over the Meso-Cenozoic with an emphasis on paleoenvironment and accumulation histories of the offshore sediments.

We show that the basins of the Guiana Shield rifted margin record (1) periods of very low siliciclastic supply concomitant with the development of carbonate platforms, alternating with (2) phases of higher siliciclastic supply associated with sand-dominated clastic deposits and turbidites. Low siliciclastic supplies reflect either very limited rift-related relief growth and erosion such as during the Central Atlantic rifting in the Late Jurassic or intense lateritic weathering of the cratonic source area during Paleogene–Miocene climate optima. Higher siliciclastic supplies correspond either to (1) periods of rapid rift-related relief growth and erosion such as during the Equatorial Atlantic rifting (Early Cretaceous), (2) periods of drainage reorganization over a steadily eroding cratonic domain (Late Cretaceous), or (3) periods of tapping of sediments stored in the Andean retro-foreland basins via the present-day Orinoco and Amazon Rivers (Plio-Pleistocene).

INTRODUCTION

Sediment routing systems shape the relief of continents by erosion and ensure the export of the sediments to the oceans where they are preserved in sedimentary basins at geological time scales (1–100 m.y.; e.g., Martinsen et al., 2010). Sediment routing systems have been studied mostly in orogenic domains because their relief, topography, and erosion rates are high and primarily driven by tectonic uplift (e.g., Métivier and Gaudemer, 1999; Clift and VanLaningham, 2010; Whittaker et al., 2011; Allen et al., 2013). Non-orogenic and cratonic domains have been less studied because their relief and erosion rates are low (Beauvais and Chardon, 2013; Grimaud et al., 2014, 2018). Nevertheless, their vast dimensions allowed them to contribute a significant proportion of the clastic sediments exported to the global ocean, which should not be underestimated in global studies (~30%–40%; Maffre et al., 2018; Milliman and Farnsworth, 2013).

Among the most studied anorogenic domains, northwestern Africa has undergone a homogeneous, slow and steady denudation at geological time scales (<7 m/m.y.; Beauvais and Chardon, 2013; Grimaud et al., 2018). The Equatorial Atlantic rifting, which achieved the separation of Africa and South America in the Early Cretaceous, impacted denudation of West Africa only locally and transiently. Indeed, the erosion of the rift-related relief took place essentially within a narrow coastal strip (100–300 km wide) of the rifted margin over a few million years after break-up that occurred at ca. 104 Ma (Wildman et al., 2019, 2022). Despite slow and steady denudation of the cratonic hinterland, accumulation in the basins of the Equatorial Atlantic rifted margin has varied significantly in time and in space (e.g., Grimaud et al., 2018). These variations must therefore primarily reflect modifications in the drainage network organization distributing sediment along the margin and/or long-term climate change. For example, the increase in accumulation rate in the Late Oligocene–Miocene was triggered by an increase in coastal catchment size due to the inland migration of the continental drainage divide (Chardon et al., 2016; Grimaud et al., 2018). This catchment reorganization was driven by the inland topographic growth of the Hoggar hot-spot swell (Chardon et al., 2016; Grimaud et al., 2018). Conversely, the very low Paleocene–early Oligocene accumulation rates recorded along the Equatorial Atlantic rifted margins of Africa reflect greenhouse climate–induced chemical weathering of the continent (Grimaud et al., 2018). Indeed, that climate favored sediment production and storage as regolith in forest-covered weathering profiles while clastic sediment exports by river systems were reduced compared to solute exports produced by chemical weathering (e.g., Fairbridge and Finkl, 1980; Tardy and Roquin, 1998; Beauvais and Chardon, 2013; Grimaud et al., 2015).

Delphine Rouby https://orcid.org/0000-0003-2827-0566

To build on these results and gain further insights into the behavior of cratonic sediment routing systems at geological time scales, their transport capacities, and controlling factors, we investigated the Guiana Shield and its Atlantic rifted margin. The northern South American cratonic domain has undergone more tectonic and epeirogenic deformation than its conjugate West African counterpart. In particular, it has been continuously bounded to the west by the active margin of the Pacific subduction since the Neoproterozoic (Torsvik and Cocks, 2013), which evolved from a paired arc–back-arc system beginning in the early Paleozoic to the Andean cordilleran orogenic system from the latest Cretaceous onward (e.g., Ramos, 1999; Fig. 1). The Atlantic rifted margin of the Guiana Shield formed in two stages: first, in the Late Jurassic, as the southern tip of the Central Atlantic rift (e.g., Klitgord and Schouten, 1986; Pindell and Kennan, 2009; Schettino and Turco, 2009) and then, in the Early Cretaceous, as part of the Equatorial Atlantic oblique rift system (e.g., Moulin et al., 2010). This polyphase history resulted in a complex three-dimensional pattern of crustal thinning along the Atlantic margin with, in particular, alternating normal and transform margin segments showing contrasting necking styles (i.e., wide normal segments and very narrow transform segments; e.g., Loparev et al., 2021). The crustal necking style, in particular the margin width, controls the amplitude and wavelength of the rift-related topography, which in turns impacts the sediment routing systems (e.g., Rouby et al., 2013; Braun, 2018). Atlantic rifting produced rift-related shoulders and marginal upwarps that divided sediment fluxes between cratonic and rifted margin basins (Bajolet et al., 2022). This configuration lasted until the Late Miocene, when the transcontinental drainage of the modern Amazon River connected the retro-foreland basin of the Andes and the Atlantic rifted margin (ca. 10–6 Ma; e.g., Hoorn et al., 2010, 2017).

Within such an evolving framework for the Meso-Cenozoic sediment routing of the Guiana Shield (Bajolet et al., 2022), the accumulation history of its outlet, the Atlantic rifted margin, remains to be established. The stratigraphic architectures of the rifted margin basins have been investigated only individually (e.g., Brandão and Feijó, 1994; Figueiredo et al., 2007; Zalán and Matsuda, 2007; Yang and Escalona, 2011; Basile et al., 2013; Sapin et al., 2016; Casson et al., 2021). The aim of the present study is to characterize, at the scale of the whole rifted margin, the stratigraphic architecture of the sedimentary basins and map their evolving paleogeography and main depocenters. This allows us to evaluate the capacity of the Guiana Shield to export sediments to the Atlantic Ocean through time and examine the consequences of the modifications of onshore sediment routing and denudation history in the offshore sedimentary record. We used an extensive set of subsurface data (two-dimensional seismic and well data provided by Total Energies) to quantify the volumetric sediment accumulation, evolving lithologies, and paleoenvironmental conditions of the offshore basins. We also estimated the denudation history of their continental source areas from published low-temperature thermochronology of the Guiana Shield (Derycke et al., 2021). We incorporated the onshore denudation and offshore accumulation histories into an integrated plate-scale kinematic and continental-crust thinning and faulting framework (after Loparev et al., 2021). Our results allow evaluation of the respective influence of the Central and Equatorial Atlantic rifting, the Andean orogenesis, and the response of the cratonic domain to long-term climate change on the organization of the sediment routing systems of the Guiana Shield toward its rifted margin since the Jurassic.

GEOLOGICAL AND GEODYNAMIC SETTINGS

The rifted margin of the Guiana Shield is located between, to the northwest, the Barbados accretionary prism forming the Caribbean subduction front (Pindell and Kennan, 2009; Yang and Escalona, 2011) and, to the southeast, the Saint Paul fracture zone (Cordani et al., 2016; Figs. 1 and 2). The northwestern portion of the margin (i.e., between the Caribbean subduction front and the Demerara Plateau) is floored by Jurassic oceanic crust accreted following rifting of the Central Atlantic (Pindell, 1985; Klitgord and Schouten, 1986; Reuber et al., 2016; Fig. 2). That portion of the margin hosts the Guiana-Suriname Basin (GS Basin). The remaining southeastern portion of the margin (i.e., between the Demerara Plateau and the Saint Paul fracture zone) is floored by Cretaceous oceanic crust formed following rifting of the Equatorial Atlantic (Moulin et al., 2010; Heine et al., 2013; Figs. 1 and 2). That portion of the margin hosts the northern and eastern Demerara basins (DEM basins) and the Foz do Amazonas Basin (FOZ Basin; Figs. 1 and 2).

Central and Equatorial Atlantic Rifting

During the Triassic and Early Jurassic (ca. 230–190 Ma), thinning of the continental crust in the study area took place at the southern tip of the Central Atlantic rift (e.g., Yang and Escalona, 2011; Ye et al., 2017; Fig. 1). This formed the GS Basin that includes a wide NNE-trending rift system at the location of the present-day Demerara Plateau and a very narrow NNW-trending rift along the present-day Guiana transform margin segment (e.g., Yang and Escalona, 2011; Casson et al., 2021; Loparev et al., 2021; Museur et al., 2021; Trude et al., 2022; Figs. 1, 2, and 3A). During the Late Jurassic and Early Cretaceous (ca. 190–130 Ma), rifting evolved to lithospheric break-up and oceanic accretion to the northwest of the Demerara Plateau (Pindell, 1985; Klitgord and Schouten, 1986; Pindell and Kennan, 2009; Schettino and Turco, 2009; Nemčok et al., 2016; Figs. 1 and 2).

In the Early Cretaceous (ca. 130–103 Ma), the Equatorial Atlantic rift system developed (Brandão and Feijó, 1994; Figueiredo et al., 2007; Zalán and Matsuda, 2007). It formed an en échelon system of dextral pull-apart basins separated by transfer faults (e.g., Mascle et al., 1988; Guiraud et al., 1992; Benkhelil et al., 1995; Basile et al., 2005; Ye et al., 2017). In the Albian (ca. 107–100 Ma), the rift system evolved to lithospheric break-up. Oceanic accretion occurred to the northeast of the Demerara Plateau (DEM basins; Mercier de Lépinay, 2016; Sapin et al., 2016; Loncke et al., 2020) and farther to the

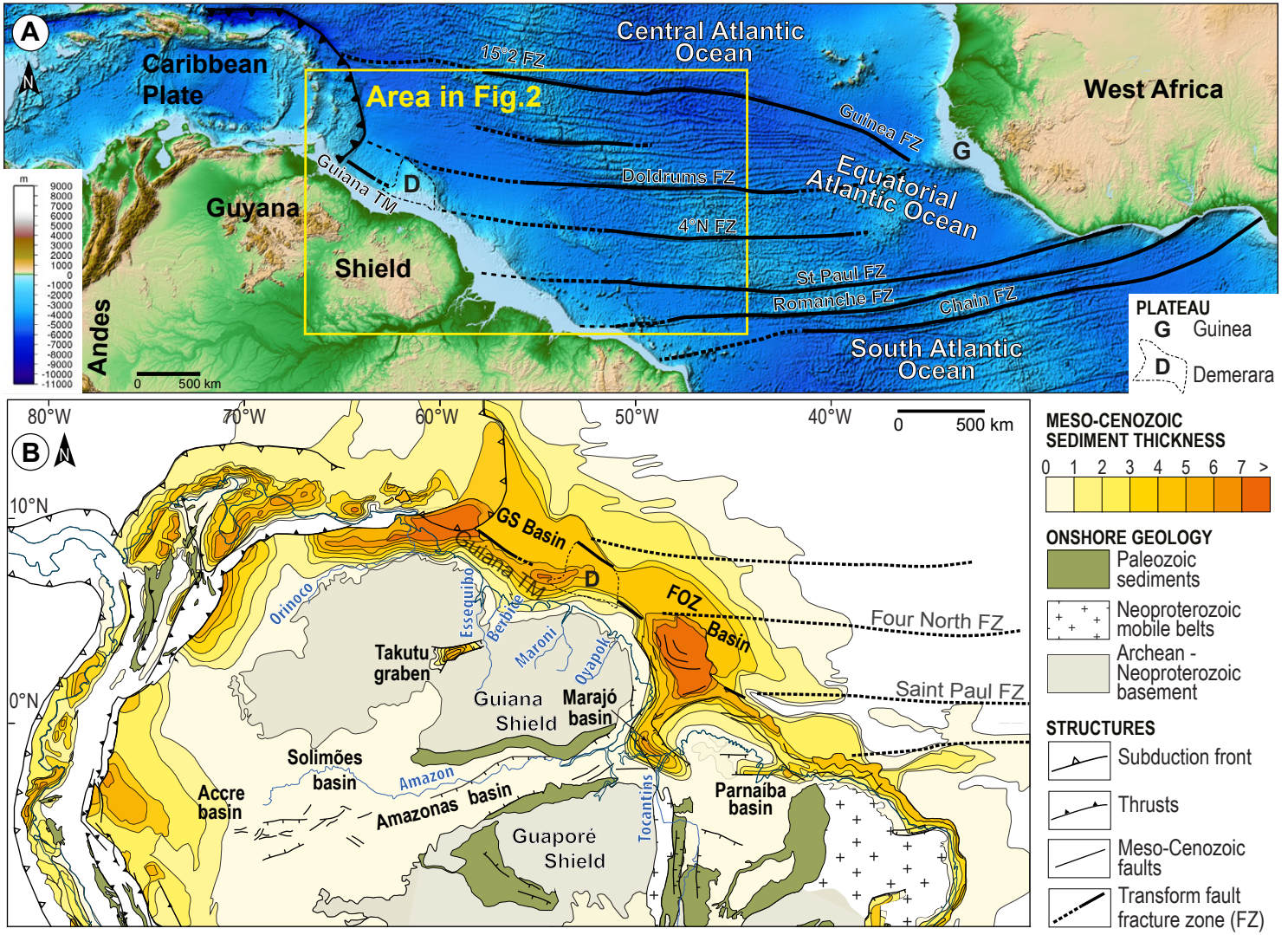

Figure 1. (A) Location of study area, northern South America. (B) Simplified geological map of northern South America and Meso-Cenozoic sediment thickness (after Cordani et al., 2016). FZ—transform fault fracture zone; TM—transform margin; GS—Guiana-Suriname; D—Demerara Plateau; FOZ—Foz do Amazonas. Topography and bathymetry after NOAA National Geophysical Data Center (2009). Modified after Loparev et al. (2021).

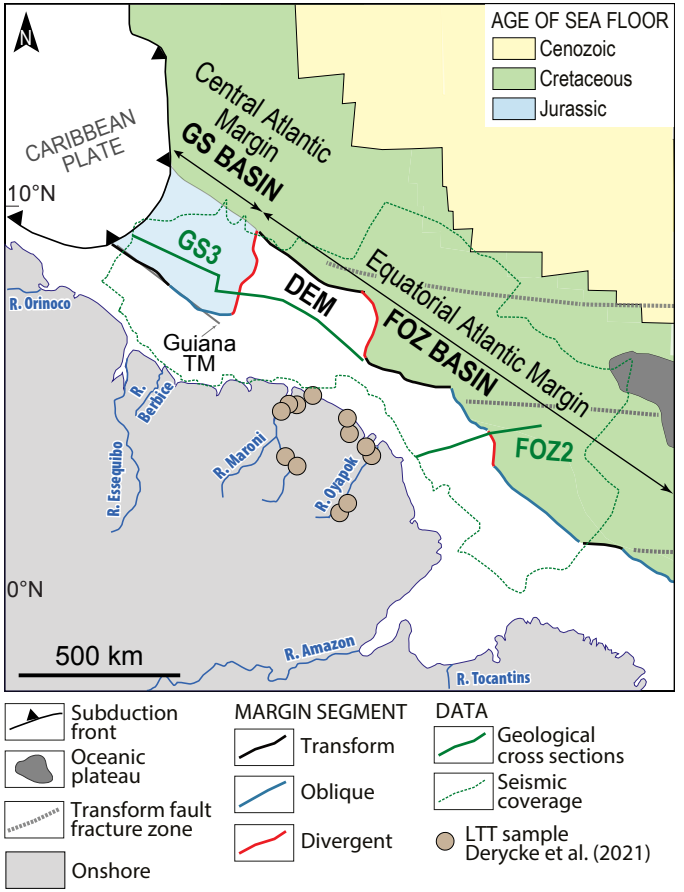

Figure 2. Location of geological sections of Figure 3 as well as areal extent of subsurface database. Samples of the low-temperature thermochronology (LTT) database are shown as open circles. GS—Guiana-Suriname; DEM—Demerara Plateau; FOZ—Foz do Amazonas; TM—transform margin. Modified after Loparev et al. (2021). Oceanic geology after Cordani et al. (2016).

southeast (FOZ basin; Brandão and Feijó, 1994; Figueiredo et al., 2007; Figs. 1 and 2). This formed isolated "oceanic crust domains" within the former pull-apart basins separated by transform or transfer faults (Basile et al., 2005; Gillard et al., 2017; Ye et al., 2017). In the Late Cretaceous (ca. 103–83 Ma), transforms accommodated further accretion and formed the equatorial part of the rifted margin.

As a consequence of the superimposition of the rifts and their obliquity, the rifted margin of the Guiana Shield shows alternating segments of variable obliquity (Basile et al., 2005; Loparev et al., 2021; Fig. 2). They can be categorized in three types depending on the angle between the segment direction and the direction of the rifting represented by directions of the transform faults: transform, oblique, and divergent segments (Ye et al., 2019; Loparev et al., 2021; Fig. 2).

Stratigraphic Architecture of the Guiana Shield Margin

The stratigraphic architecture of the GS Basin first receives the Central Atlantic syn-rift deposits that form a wide volcaniclastic depocenter below the present-day Demerara Plateau divergent margin segment and much thinner deposits along the transform-oblique segment (Figs. 2 and 3A; Casson et al., 2021; Loparev et al., 2021; Trude et al., 2022). The syn-rift infill is truncated by the Central Atlantic break-up unconformity, above which an Upper Jurassic carbonate platform developed along the eastern boundary of the syn-rift basin (Fig. 3A; e.g., Yang and Escalona, 2011; Mercier de Lépinay, 2016; Casson et al., 2021; Loparev et al., 2021). Above that unconformity, Cretaceous post-rift clastic systems, which are widely spread from the proximal to the oceanic domains, show a long-term aggrading trend and depocenters progressively migrating into the distal margin domain and onto the oceanic crust (Fig. 3A). Thin Paleogene and Miocene deposits indicate a reduced clastic input to the GS Basin between ca. 66 and 6 Ma. Sedimentation resumed in the Pliocene and deposits are significantly thicker (Fig. 3A; Yang and Escalona, 2011; Loparev et al., 2021). Indeed, they are fed not only by Berbice River but mostly by the Orinoco River whose outlet followed Caribbean trench eastward retreat and routed sediments from the Andean retro-foreland to the GS Basin (Fig. 1B; e.g., Yang and Escalona, 2011; Loparev et al., 2021).

The stratigraphic architecture of the DEM and FOZ basins comprises Early Cretaceous thin and narrow clastic syn-rift deposits under continental and shallow marine depositional environments (Fig. 3B; e.g., Mercier de Lépinay, 2016; Sapin et al., 2016; Loparev et al., 2021). These deposits are truncated by the Equatorial Atlantic break-up unconformity above which post-rift deposits are widely spread from the proximal to the oceanic domain (Fig. 3B; e.g., Mercier de Lépinay, 2016; Sapin et al., 2016; Loparev et al., 2021). Upper Cretaceous deposits first filled up existing relief and then evenly spread over the entire margin width. From the Paleogene onward, deposits became thicker in the oceanic domain than in the proximal domain (Fig. 3B; e.g., Loparev et al., 2021). During the Paleogene and Miocene, the margin was starved of clastic influx, allowing for the development of a wide carbonate platform (e.g., Carozzi, 1981; Figueiredo et al., 2007; Sapin et al., 2016; Loparev et al., 2021). The clastic input was renewed in the Pliocene, with a platform delta fed by the Maroni River on the Demerara Plateau (Fig. 3B) and, mostly, the giant Amazon Delta burying the carbonate platform under very thick clastic series (Figs. 1 and 3B; e.g., Hoorn et al., 1995, 2010; Watts et al., 2009; Shephard et al., 2010; van Soelen et al., 2017). The delta formed after the establishment of the modern course of the Amazon River in the Late Miocene, routing sediments from the

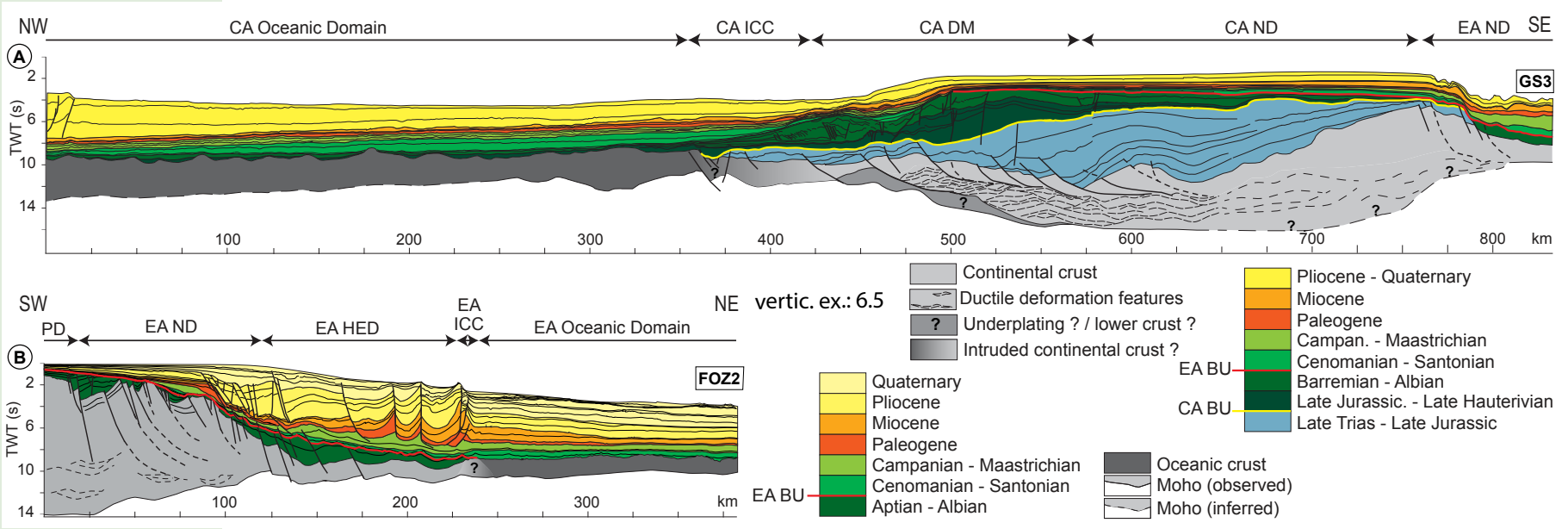

Figure 3. (A) Geological cross-section GS3 (Guiana-Suriname [GS] Basin and East Demerara). (B) Geological cross-section FOZ2 (Foz do Amazonas [FOZ] Basin). See location on Figure 2. TWT—two-way travel time; CA—Central Atlantic; EA—Equatorial Atlantic; ICC—intruded continental crust; DM—distal margin; ND—necking domain; PD—proximal domain; HED—hyper-extended domain; BU—break-up unconformity. Vertic. ex.—vertical exaggeration. Trias—Triassic. Modified after Loparev et al. (2021).

Andean retro-foreland across the Amazonian plains to the FOZ Basin (Hoorn et al., 1995, 2010; Shephard et al., 2010; van Soelen et al., 2017).

METHOD

Data Set

To determine the sedimentary history of the rifted margin basins, we interpreted a dense grid of industrial seismic reflection profiles (between the Caribbean subduction front and the Saint Paul fracture zone; extent of data set on Fig. 2 and data set map on Fig. S1 in the Supplemental Material[1]). We calibrated our seismic interpretations and sedimentary facies using 33 exploration wells (located in the shelf and bathyal domains; Fig. S1). To estimate the denudation history of the Guiana Shield at the regional scale, we used the published thermal history of Derycke et al. (2021) established from inversions of low-temperature thermochronology (LTT) data coupling apatite fission tracks and (U-Th)/He dating (location of samples in Fig. 2).

[1]Supplemental Material. Text file with additional method information including six figures and six tables. PowerPoint file with eight slides with isopach, paleoenvironment, and lithologic maps organized for each period. Please visit https://doi.org/10.1130/GEOS.S.22223389 to access the supplemental material, and contact editing@geosociety.org with any questions.

Isopach Maps

We mapped nine stratigraphic horizons across the studied area (Fig. S3) using seismic and sequence stratigraphy methods (see details in Section S2.1 [see footnote 1]; Figs. S5 and S6). We illustrate the margin geometry by two interpreted cross sections (Fig. 3). Additional cross sections can be found in the Supplemental Material (Figs. S3 and S4). From the nine horizon maps, we constructed eight isochore maps in two-way travel time that we depth-converted into thickness maps. Details on the depth-conversion can be found Section S2.2. Note that for the Central Atlantic syn-rift and early post-rift intervals (200–165 Ma), evaluated thicknesses are minimal values because the volcanic content of these deposits is unknown. We integrated the isopach maps within a plate kinematic and crustal thinning framework provided by the reconstructions of Ye et al. (2017), Loparev et al. (2021), and Bajolet et al. (2022) (Fig. 4).

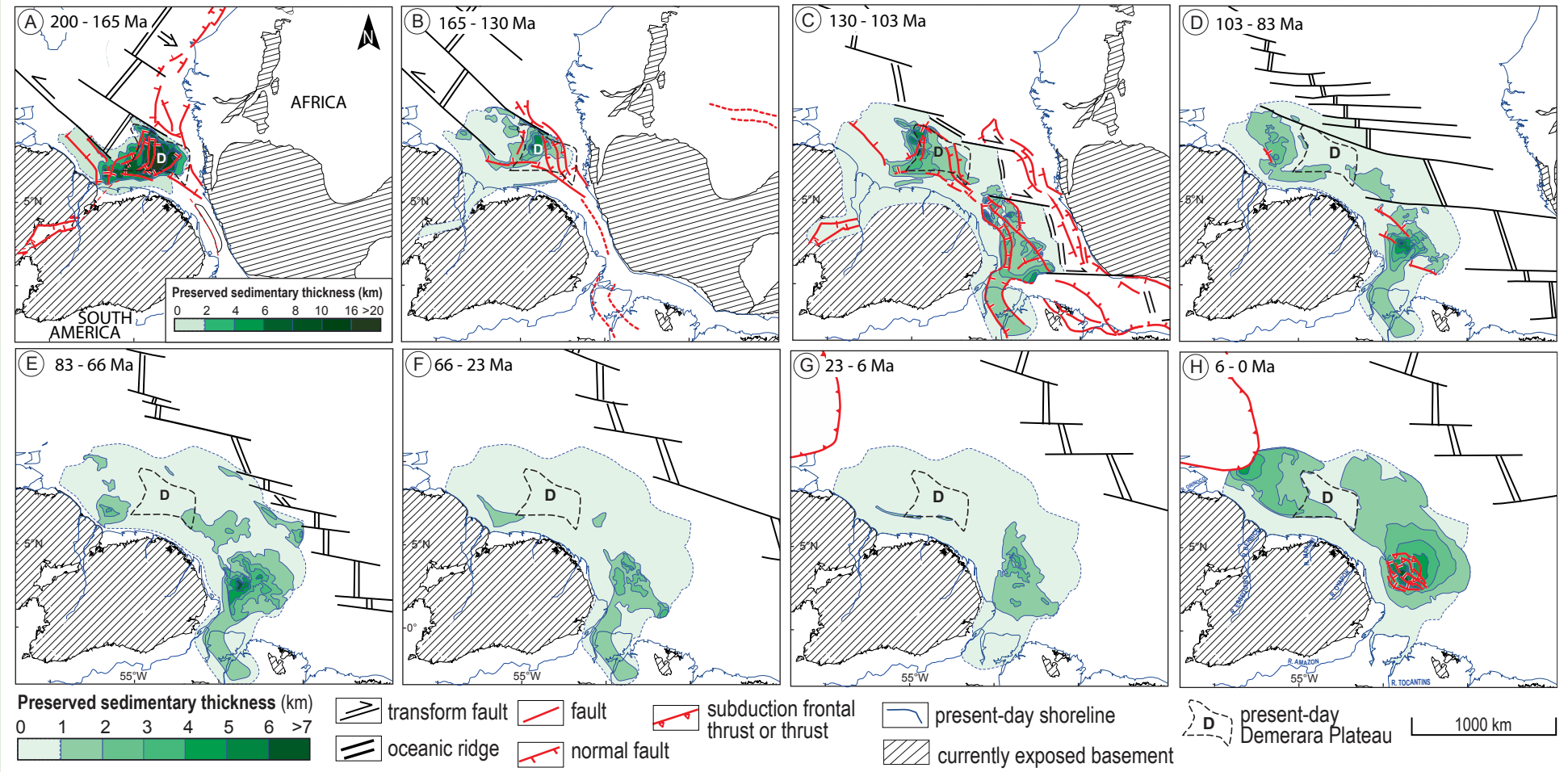

Figure 4. Accumulation maps of the study area established from seismic data. (A) 200–165 Ma: Central Atlantic rifting, break-up, and accretion. (B) 165–130 Ma: Central Atlantic post-rift. (C) 130–103 Ma: Central Atlantic post-rift and Equatorial Atlantic rifting, break-up, and accretion. (D–H) 103–0 Ma: Central and Equatorial Atlantic post-rift. Note that during Central Atlantic syn-rift and early post-rift phases (200–165 Ma), sediment thicknesses have been depth converted assuming terrigenous deposit velocities; they are therefore minimum thicknesses.

That framework includes the position of the landmasses at the end of each considered interval and the main active faults (Fig. 4).

Accumulated Solid Siliciclastic Volumes and Rates

For each isopach map, we calculated the raw incremental volumes of sediments accumulated in the GS and FOZ basins. We followed the method of Rouby et al. (2009) to correct the raw volumes from remaining porosity and in situ production (carbonates or volcanics) and compute solid siliciclastic volumes (Figs. 5A–5C). Details of the approach can be found in Sections S2.3 and S2.4 (Fig. S6, see footnote 1). We calibrated the horizons in absolute ages to calculate incremental volumetric accumulation rates (Figs. 5D–5F; Section S2.5). We also estimated the variability of the results due to the uncertainties in the calibration of horizons in absolute ages, the depth conversion, and the corrections for porosity and in situ carbonate production using the method of Guillocheau et al. (2012; Fig. 5). Details of uncertainty estimation can be found in Section S2.6.

Paleoenvironment Maps

From the seismic and sequence stratigraphy interpretation of the subsurface data set, we constructed depositional environment maps for each time interval (Fig. 6). We mapped fluvial, coastal, and deltaic plain facies as continental environments, continental platform facies as transitional environments, bathyal facies (continental slope) as shallow marine environments (<200 m), and abyssal facies as deep marine environments (>200 m). On the continent, sedimentary paleoenvironments are represented by the area of preserved deposits (dark colored in Fig. 6) and the minimal areal extent beyond that preserved area at the time of deposition (light colored in Fig. 6) (after Ye et al., 2017; Bajolet et al., 2022). Note that for the 200–165 Ma interval, we mapped

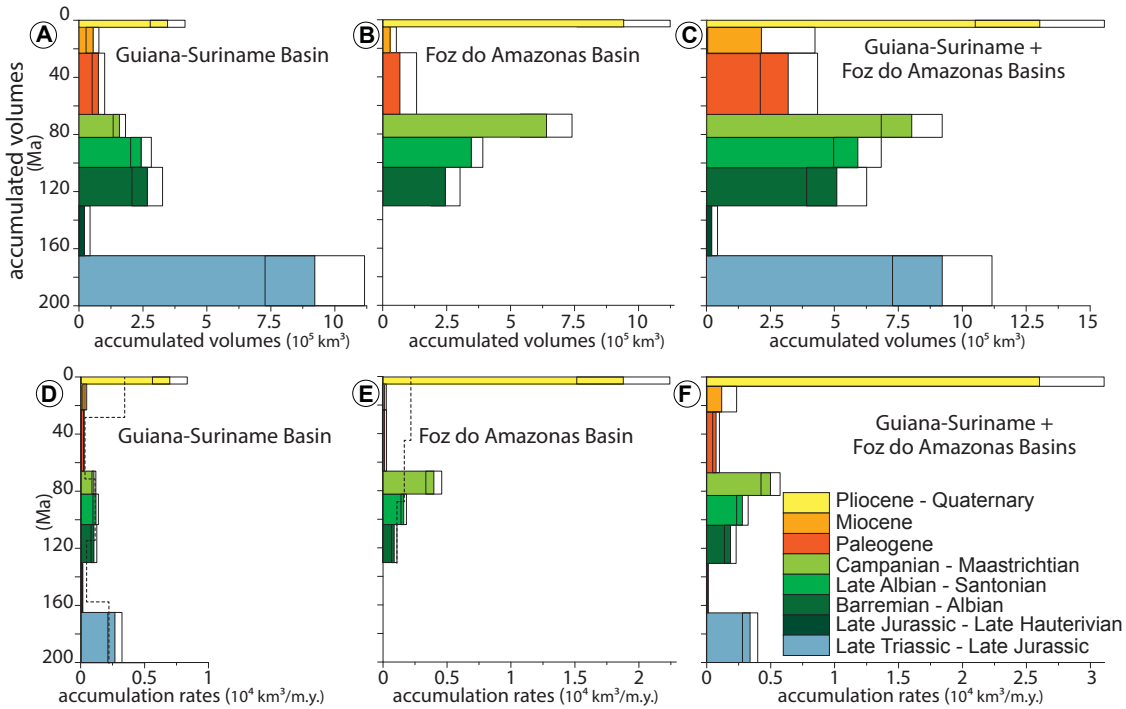

Figure 5. Solid siliciclastic accumulated volumes and accumulation rates in the Guiana-Suriname Basin (A and D), Foz do Amazonas Basin (B and E), and both basins cumulated (C and F). Uncertainties are shown by black boxes. Note that for the 200–165 Ma interval, values are minimums (unknown volcanic/clastic ratio in syn-rift deposits). Dashed lines for accumulation rates in D and E are accumulation rates resampled using even time increments.

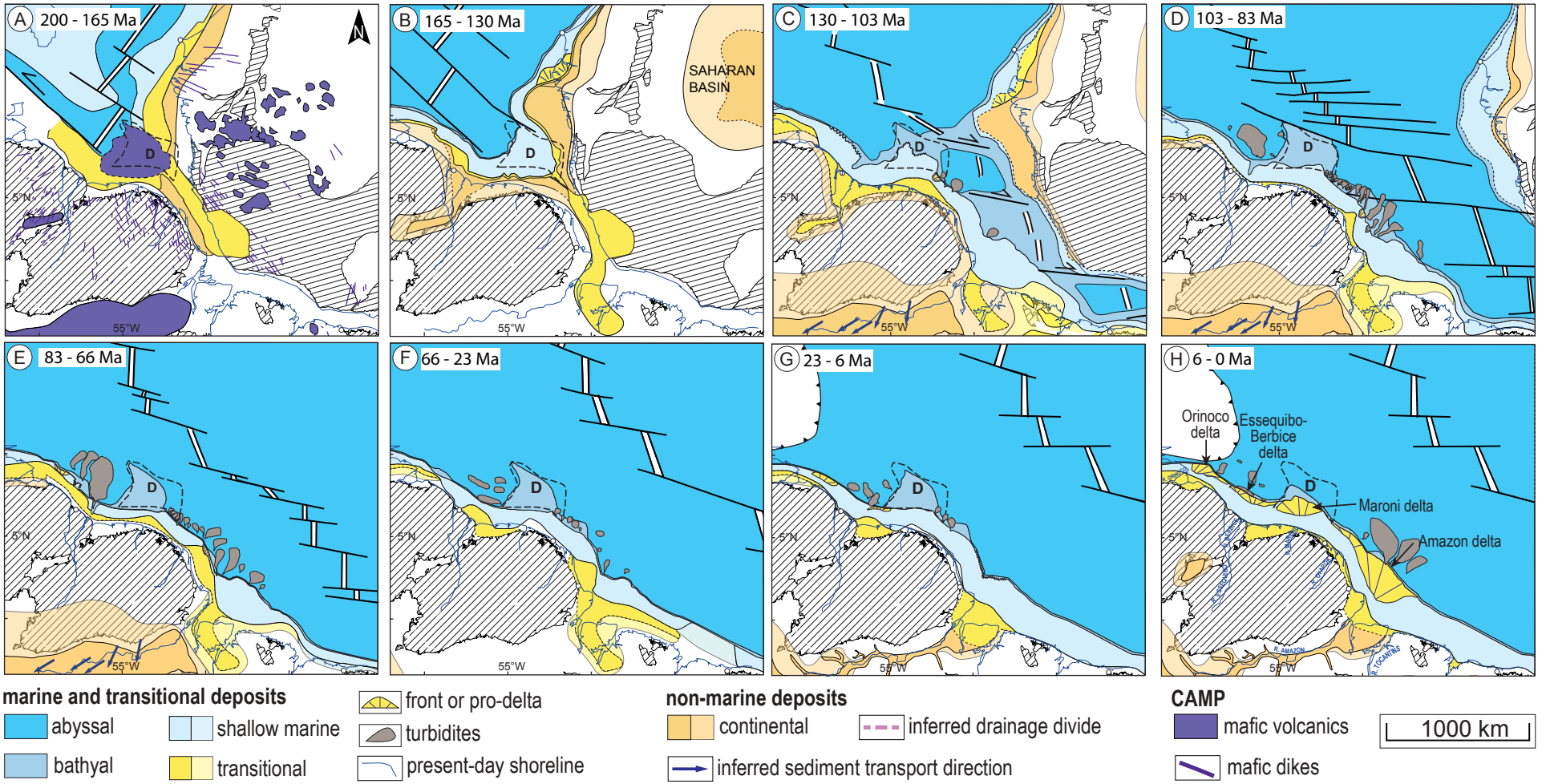

Figure 6. Paleoenvironment maps of the study area. (A) 200–165 Ma: Central Atlantic rifting, break-up, and accretion. (B) 165–130 Ma: Central Atlantic post-rift. (C) 130–103 Ma: Central Atlantic post-rift and Equatorial Atlantic rifting, break-up, and accretion. (D–H) 103–0 Ma: Central and Equatorial Atlantic post-rift. Note that for the 200–165 Ma interval, we mapped occurrences of volcanics (unknown volcaniclastic ratio content) in the syn-rift deposits. Drainage divides and sediment transport direction are from Bajolet et al. (2022). For continental, transitional, and shallow marine deposits, the darker shade corresponds to the present-day extent of preserved deposits and the lighter shade corresponds to the estimated minimum initial extension of the deposits. CAMP—Central Atlantic magmatic province. Additional symbol explanation can be found in Figure 4.

occurrences of volcanics in the syn-rift depocenter although the volcanic and clastic content is unknown (Fig. 6A). We used Ye et al. (2017) for the African rifted margin paleoenvironment reconstructions. Additional details of the mapping criteria and method can be found in Section S3 (see footnote 1).

Paleo-Lithology Maps

We also constructed maps of main lithologies (Fig. 7). We defined six types of dominant lithology: sand (sand content >90%, usually the fluvial, coastal, and deltaic plain), sand-clay (sand content >60%), clay-sand (sand content <40%), shale (sand content <10%, usually the abyssal domain), carbonates (usually the platform domain), and marl (usually deposits in bathyal environments at the toe of carbonate platforms). We calibrated lithologies on well data (Fig. S3). For the 200–165 Ma interval, we mapped the syn-rift depocenter of the Central Atlantic rift although its volcanic/clastic ratio remains unknown (Fig. 6A). Additional details of the mapping criteria and method can be found in Section S3 (footnote 1).

Denudation History

We selected the published preferred thermal history of model of Derycke et al. (2021) from the inversion of LTT dating for six series of samples (see location on Fig. 2). Following the method of Wildman et al. (2019), we assumed that onshore sample cooling or heating was primarily driven by unroofing or burial and chose a constant paleo–thermal gradient of 25 °C/km (geothermal gradient within the first 3–5 km of Earth's surface in a normal continental crust; DiPietro, 2013).

We derived the denudation/burial from thermal history using:

$$D = (T_1 - T_2) / G, \quad (1)$$

$$d = D / (t_1 - t_2), \quad (2)$$

where D is denudation (km), d is denudation rate (km/m.y.), T_1 and T_2 are the expected temperatures (°C) at time t_1 and time t_2 (Ma), and G is the geothermal gradient (°C/km). We also used the 95% confidence interval of the thermal histories of Derycke et al. (2021) to estimate the uncertainties in denudation and burial estimations (Fig. 8). Denudation and burial values and associated uncertainties can be found in Table S6 (see footnote 1).

RESULTS

We organized our results for visualizing the spatial and temporal evolution of depocenters (Fig. 4), accumulation history (Fig. 5), depositional environments (Fig. 6), main lithologies (Fig. 7), and denudation history of the cratonic domain (Fig. 8). The paleomaps of Figures 4, 6, and 7 are arranged by time intervals from panel A to panel H. We also provide in PowerPoint File S1 (see footnote 1) an alternative presentation of the maps, with depocenters, depositional environments, and lithologies shown together on a same figure for a given time interval.

Central Atlantic Syn-Rift and Early Post-Rift (200–130 Ma)

Between 200 and 165 Ma, crustal deformation was driven by the Central Atlantic rifting and early post-rift phases (Fig. 4A). The main depocenter is very thick (at least 20 km) and occupies a wide rift zone that formed below the present-day Demerara Plateau (Fig. 4A). The associated volume is at least 9 × 10^5 km^3, including an unknown proportion of volcanics (200–165 Ma interval; Fig. 5A). Besides this volcaniclastic syn-rift infill, depositional environments are continental to transitional (Fig. 6A). Deposits are clastic (clay-sand) along the South American rifted margin (Fig. 7A). In contrast, a carbonate platform developed along the African part of the rifted margin (Fig. 7A). This is consistent with little clastic input to that part of the margin at the time, although no data are available for its clastic accumulation history. To the northwest of the study area, the Central Atlantic break-up and oceanic accretion took place. The associated distal basin developed under shallow and deep marine depositional environments (shale dominated; Figs. 6A and 7A). Inland, the SE-trending rift branch separating the Guiana Shield and the West African craton, as well as the Marajó Basin, received sand-clay deposits under fluvio-deltaic environments (Figs. 6A and 7A).

After Central Atlantic rifting (165–130 Ma), the main depocenter remained below the present-day Demerara Plateau but spread northwestward to the distal part of the rifted margin (Figs. 3A and 4B). It was also much thinner (<7 km) than during the previous time interval (Figs. 3A, 4A, and 4B). A continuous strip of transitional depositional environments continuously fringed the rifted margin in Africa and northern South America (Fig. 6B). That strip mostly coincides with a carbonate platform (Fig. 7B). This is consistent with the very low clastic input to the margin at the time (165–130 Ma interval; ~0.2 × 10^2 km^3 and 60 km^3/m.y.; Figs. 5A and 5D). In the distal domain of the rifted margin, depositional environments have remained deep marine (shale dominated) until the present day (Figs. 6B–6H and 7B–7H).

Equatorial Atlantic Syn-Rift and Early Post-Rift (130–66 Ma)

Between 130 and 103 Ma, crustal deformation was due to the Equatorial Atlantic rifting (syn-rift and early post-rift) in the DEM and FOZ basins (Fig. 4C). Accordingly, in the GS Basin, only normal faults restricted to the sedimentary cover were active, mostly accommodating collapse of the platform, westward along the divergent margin segment and northward along the

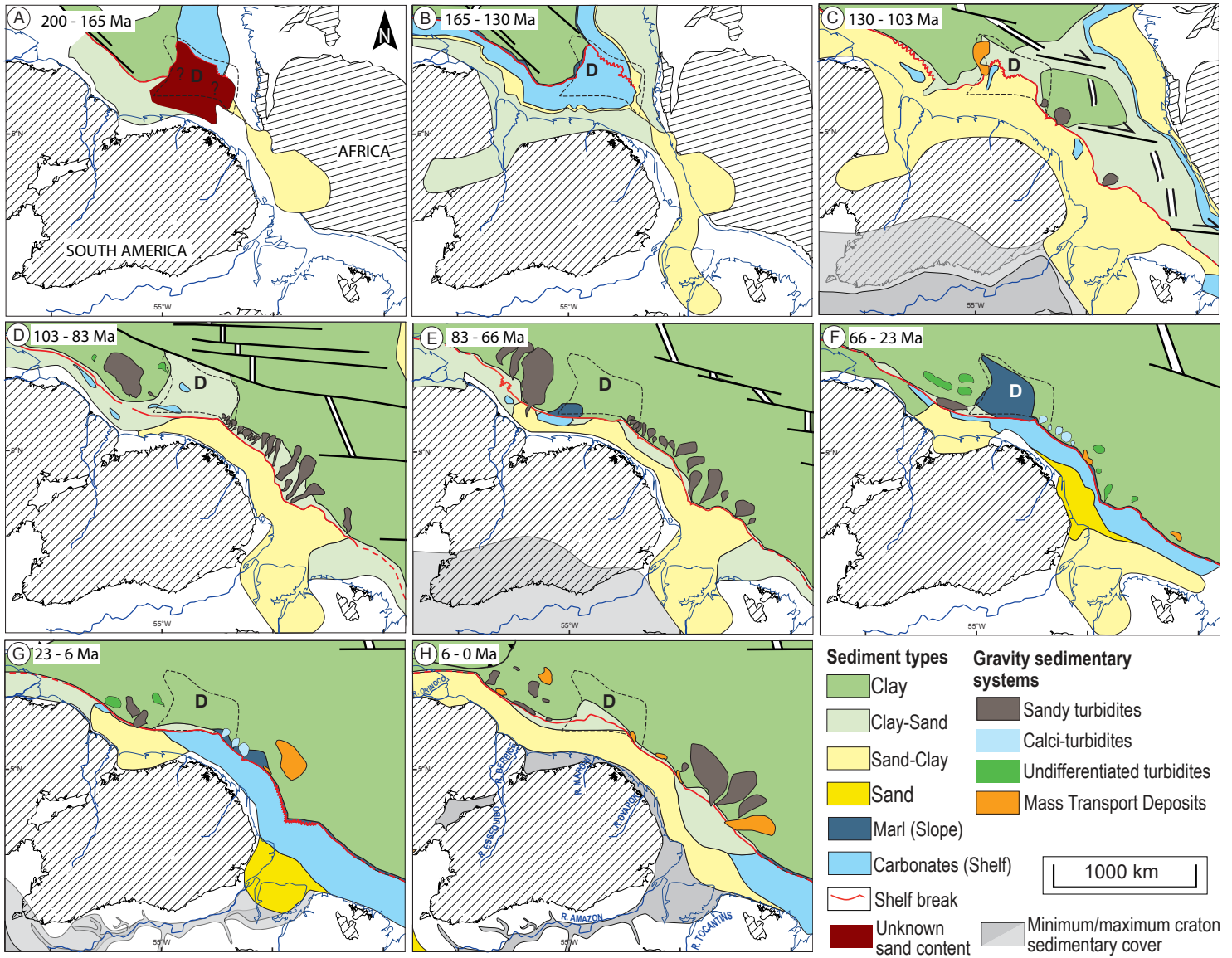

Figure 7. Lithologic maps of the study area. (A) 200–165 Ma: Central Atlantic rifting, break-up, and accretion. (B) 165–130 Ma: Central Atlantic post-rift. (C) 130–103 Ma: Central Atlantic post-rift and Equatorial Atlantic rifting, break-up, and accretion. (D–H) 103–0 Ma: Central and Equatorial Atlantic post-rift. Note that for the 200–165 Ma interval, the volcano/clastic ratio is unknown in the syn-rift sediments. Additional symbol explanation can be found in Figure 4.

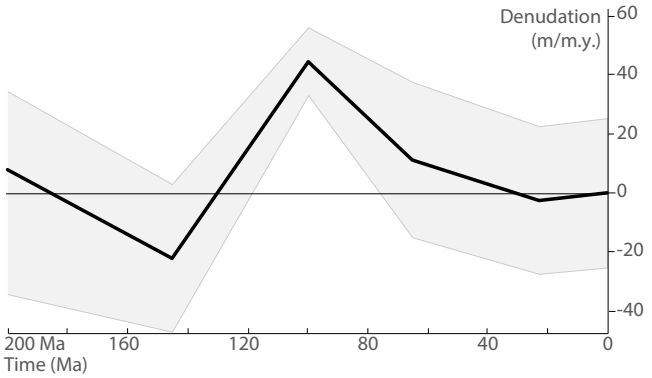

Figure 8. Denudation history of Guiana Shield (after low-temperature thermochronology data of Deryck et al., 2021). Black line corresponds to inversion of the six series of samples (see location on Fig. 2). Shaded area corresponds to the associated uncertainties (i.e., the 95% confidence interval). Negative denudation corresponds to burial. See location of samples in Figure 2. Values can be found in Table S6 (see footnote 1).

oblique-transform margin segment (Loparev et al., 2021; Figs. 2, 3A, and 4C). The main depocenter shifted westward into the eastern GS Basin (Figs. 3A and 4C). In the Equatorial Atlantic rifting domain (DEM and FOZ basins), depocenters were controlled by en échelon dextral pull-apart basins formed in between the Guiana Shield and West African craton (Fig. 4C). Farther south, the Marajó rift received sediments as well (Fig. 4C). The clastic supply initiated in the DEM and FOZ basins was renewed in the GS Basin (130–103 Ma interval; Figs. 5A and 5B). Deposits in fluvial-deltaic and transitional environments (sand-clay) covered most of the previous carbonate platform except in a few local patches (Figs. 6C and 7C). The African conjugated margin showed more pronounced continental environments (sand-clay deposits) fringed oceanward by a very narrow carbonate platform (Fig. 7C). The Equatorial Atlantic rift domain was under shallow environments with clay-sand deposits except in the newly formed isolated patches of oceanic crust that reach abyssal environments with shale-dominated deposits (Figs. 6C and 7C).

Between 103 and 66 Ma, crustal thinning ceased and separation of the Guiana Shield and the West African craton became accommodated by accretion and transform faults (Figs. 4D and 4E). Only very local and limited gravity-driven deformation occurred in the main depocenters of the GS and FOZ Basins between 103 and 83 Ma and ceased afterwards (Loparev et al., 2021; Figs. 4D and 4E). Volumes of clastic sediment accumulated in the GS Basin decreased over the Late Cretaceous (from ~2.7 to ~1.6 × 10^5 km^3) while they increased in the FOZ Basin (from ~2.4 to ~6.5 × 10^5 km^3; 103–66 Ma interval; Figs. 5A and 5B). The Guiana Shield rifted margin was dominated by transitional and bathyal environments (Figs. 6D and 6E). Except for a few isolated patches of carbonates, deposits were clastic with higher sand contents in the proximal domain of the FOZ Basin (sand-clay) than in the GS Basin (clay-sand; Figs. 7D and 7E). During that period, turbiditic systems developed, in particular at the junction of the oblique and normal margin segments in the GS Basin and in the FOZ Basin (Figs. 2, 7D, and 7E). These systems exported sand-dominated deposits across the shelf break from the platform to the shale-dominated abyssal plain (Figs. 7D and 7E).

Thus, after Equatorial Atlantic break-up, the Guiana rifted margin was dominated by clastic sedimentation with depocenters controlled by post-rift subsidence as well as the main river outlets (Figs. 4D–5E, 6D–6E, and 7D–7E). In the GS Basin, the main depocenter was fed by sediment routed through the intersection between the oblique and divergent segments, potentially from the Essequibo, Berbice, and/or Maroni Rivers or their ancestors (Figs. 2B, 4D, and 4E). In the DEM and FOZ basins, the main depocenter was fed by sediments routed through the former Marajó rift, probably from a paleo–Tocantins and paleo–Oyapok Rivers (Figs. 4D and 4E).

Equatorial Atlantic Late Post-Rift (66–0 Ma)

Between 66 and 6 Ma, clastic accumulation was very limited (66–6 Ma interval; Fig. 5). The proximal domains of the GS Basin and the Demerara Plateau underwent marl- or shale-dominated deposition while a carbonate platform was installed in the FOZ Basin (Figs. 6F, 6G, 7F, and 7G). The number of turbiditic systems decreased drastically with respect to the Late Cretaceous (Figs. 7F–7H). Only small calci-turbiditic lobes were emplaced in the abyssal plain east and west of the Demerara Plateau (Figs. 7F and 7G) as well as a few sand lobes at the transition between the oblique and divergent margin segments of the GS Basin (Figs. 7F and 7G).

Between 6 and 0 Ma, clastic supply to the margin drastically increased through the Amazon, Maroni, Essequibo-Berbice, and Orinoco deltas (66–6 Ma interval; Figs. 4H, 5, and 6H) following establishment of the transcontinental drainage linking the Andean retro-foreland to the Atlantic rifted margin by the modern Amazon River and Orinoco River systems (between 10 and 6 Ma; Hoorn et al., 1995, 2010; Shephard et al., 2010; van Soelen et al., 2017). Accumulations were mostly clastic in fluvial and transitional depositional environments (sand-clay and clay-sand facies). These deposits covered the former carbonate platform except at the southeastern tip of the study area (Figs. 6H and 7H). Turbiditic export resumed in the FOZ Basin (Fig. 7H).

Denudation History of the Guiana Shield

The six batches of LTT samples are located within 300 km of the Guiana Shield rifted margin (Fig. 2). Overall, the samples show heating between 200 and 145 Ma (burial rate as high as –35 m/m.y.), rapid cooling between 145 and 100 Ma (denudation rate of 30 to 60 m/m.y.), and very slow and steady cooling afterwards (denudation rate of <20 m/m.y. or burial; Fig. 8).

Derycke et al. (2021) related the heating trend between 200 and 140 Ma ("burial" on Fig. 8) to a Central Atlantic magmatic province (CAMP)–related magmatism heating rather than to burial. However, heating overlaps with the Central Atlantic rifting (ca. 230–165 Ma). Basile et al. (2020) suggested that the magmatic activity of this rifting might have been related to a hot spot (ca. 170–180 Ma). This could provide an alternative origin for this heating episode. The following increase in denudation rates between 145 and 100 Ma (to as much as ~40 ± 10 m/m.y.; Fig. 8; Table S6 [see footnote 1]) is coeval with the Equatorial Atlantic rifting. It is interpreted by Derycke et al. (2021) as due to the erosion of the rift-related relief (Figs. 4C and 8).

After ca. 90–100 Ma, samples were at <2 km depth, implying a less constrained thermal history because they recorded temperature too low to be interpreted as due to denudation or burial (Derycke et al., 2021). Paleogene (>30 Ma) lateritic weathering profiles are currently preserved over most of the Guiana Shield (Théveniaut and Freyssinet, 2002). Their formation since probably the Late Cretaceous and their current preservation are consistent with limited denudation (<10 m/m.y.) or burial of the shield since ca. 70 Ma Fig. 8; Table S6). This is also consistent with estimations of denudation made for the same period for the conjugated West African craton from both thermochronological and geomorphological data (Beauvais et al., 2008; Grimaud et al., 2018; Wildman et al., 2019, 2022).

DISCUSSION

Contrasted Sedimentary Records of Central and Equatorial Atlantic Rifting (200–103 Ma)

The accumulation history of the Guiana Shield margin is controlled primarily by the rifting of the Central Atlantic in the Early–Middle Jurassic (200–165 Ma; Fig. 4A) and of the Equatorial Atlantic in the Early Cretaceous (130–103 Ma; Fig. 4C). The contrasted crustal and stratigraphic architectures of the associated basins along the Guiana Shield rifted margin show that the Central Atlantic and Equatorial Atlantic rifts resulted from very different types of crustal thinning processes (Fig. 3).

For instance, the Central Atlantic syn-rift depocenter is much larger than the Equatorial Atlantic syn-rift depocenter (>9 × 10^5 km^3 and 2.5 × 10^5 km^3 respectively; Figs. 3, 4A, 4C, 5A, and 5B). Also, the Central Atlantic syn-rift deposits include an unknown but probably large proportion of volcanics (i.e., seaward-dipping reflectors; Fig. 7A) while the Equatorial Atlantic syn-rift deposits do not (Fig. 7C). Additionally, the thermal history of the Guiana Shield suggests that Central Atlantic rifting was coeval with a heating episode, tentatively related to a magmatic event (CAMP or hot spot), while Equatorial Atlantic rifting was coeval with a cooling episode related to the erosion of the rift-related relief. Finally, the Central Atlantic rifting has involved a larger proportion of ductile deformation during thinning than the Equatorial Atlantic rifting (e.g., Loparev et al., 2021; Museur et al., 2021).

In terms of depositional environments (outside the volcanic depocenter), syn-rift clastic deposits of the Central Atlantic are finer grained (clay-sand; Fig. 7A) than the Equatorial Atlantic syn-rift deposits (sand dominated; Fig. 7C). This suggests that the Equatorial Atlantic syn-rift sediments resulted from the erosion of steeper rift-related reliefs than the Central Atlantic syn-rift sediments. Furthermore, in the Central Atlantic domain (165–130 Ma; Fig. 4B), a wide carbonate platform developed immediately after the break-up (Fig. 7B), while accumulated clastic volumes were extremely low (Figs. 4B, 5A, 5D). This suggests that the rift-related reliefs were mostly eroded away immediately after break-up and/or too low to provide a significant clastic supply to the Central Atlantic rifted margin (Figs. 4B, 5A, 5D, and 7B). By contrast, along the Equatorial Atlantic rifted margin, large volumes of sand-dominated deposits associated with turbiditic systems accumulated throughout the Late Cretaceous (i.e., during rifting, break-up, and early post-rift; 103–66 Ma; Figs. 5B, 5E, and 7C–7E). This suggests that Equatorial Atlantic rifting formed a relief (upwarp) high and persistent enough to sustain an entrenched drainage delivering coarse-grained clastics to the Equatorial Atlantic rifted margin for 40 m.y. after break-up. This drainage also allowed renewal of the clastic supply to the GS Basin (former Central Atlantic rifting) throughout the Late Cretaceous (i.e., 100 m.y. after the Central Atlantic rifting), burying the former carbonate platform under sand-dominated and clay-dominated deposits (Figs. 7C–7E). To summarize, the Equatorial Atlantic rift-related relief (and drainage system) sustained a larger, coarser-grained, and longer-lasting clastic supply (>40 m.y. after rifting) than that feeding the Central Atlantic rift, which was eroded away immediately after rifting (Figs. 4A, 5A, and 7B).

These differences in the types of crustal deformation and rift-related reliefs may be related to the contrasted kinematic developments of the two rifts. Indeed, the Equatorial Atlantic rifting was faster and more oblique than the Central Atlantic rifting (Brune et al., 2016, 2018). Faster and more oblique rifts produce a narrower rifted margin with higher rift-related relief than slower and normal rifts (e.g., Svartman-Dias et al., 2015; Theunissen and Huismans, 2019; Wolf et al., 2022). This is also consistent with the Central Atlantic rifting involving a larger proportion of ductile deformation during thinning than the Equatorial Atlantic rifting (e.g., Loparev et al., 2021). Indeed, a weaker and/or warmer lithosphere generates lower rift relief than a colder lithosphere (e.g., Beucher and Huismans, 2020; Wolf et al., 2022).

In terms of source to sink, the sand content and hence the siliciclastic volume of sediments produced by rifting of the Central Atlantic is unknown. However, the Equatorial Atlantic rift preserved a solid volume of ~5 ± 1.9 × 10^5 km^3 between 130 and 103 Ma (Fig. 5; Table S5 [see footnote 1]). This volume is at first order consistent with the ~1.5 km of unroofing recorded by LTT data of Derycke et al. (2021) between 130 and 100 Ma if generalized to the area of the Guiana Shield (~500 × 500 km; Table S6).

Overall, the Equatorial Atlantic rift-related relief sustained a larger, coarser-grained, and longer-lasting clastic supply than the relief feeding the Central Atlantic rift, whose relief was eroded away rapidly after rifting. One would therefore expect larger, coarser-grained, and longer-lasting clastic supply in

narrow and fast oblique rifts than in wider and magmatic rifts. Nevertheless, in the study area, the Central Atlantic and Equatorial Atlantic rifts were superimposed, and the relative contribution of Central Atlantic rifting inheritance on relief dynamics of Equatorial Atlantic rifting remains to be evaluated.

A Late Cretaceous Clastic-Dominated Rifted Margin (103–66 Ma)

After Equatorial Atlantic break-up, the Guiana rifted margin was dominated by clastic sedimentation, with depocenters controlled by post-rift subsidence as well as the main river outlets (Figs. 4D–4E, 6D–6E, and 7D–7E). Unroofing of the Guiana Shield remained low, steady, and spatially evenly distributed (Fig. 8). Meanwhile, the accumulated sediment volumes and accumulation rates increased during the Late Cretaceous (Figs. 5C and 5F). But the accumulation trends differ in the GS and FOZ Basins: Accumulated volumes and accumulation rates increased in the FOZ Basin, while accumulated volumes decreased and accumulation rates remained steady in the GS Basin (Figs. 5A, 5B, 5D, and 5E). Given the bulk steady unroofing of the Guiana Shield, this contrast in accumulation history cannot be related to an increase in rock uplift in the source area, whether driven by tectonics or mantle dynamics. Nor can it be related to a change to a climate more propitious to physical erosion given that the two basins show opposite accumulation trends. It therefore most probably results from change(s) in the organization of the drainage feeding the rifted margin. Few geologic data are available to further constrain such modifications. But several authors have suggested that the drainage supplying the GS Basin during the Early Cretaceous included the Takutu graben (McConnell, 1969; Crawford et al., 1985; Roddaz et al., 2021; Bajolet et al., 2022; Trude et al., 2022; Fig. 9). This implies that a drainage longer than at present day would have contributed to renewing siliciclastic accumulations in the GS Basin after ca. 145 Ma (Figs. 5A and 7C–7E). To account for the following decrease in accumulation (ca. 145–66 Ma; Fig. 5A), we suggest that the drainage area decreased in the Late Cretaceous, i.e., the watershed, initially located south of the Takutu graben, migrated oceanward (Fig. 9). Nevertheless, the mechanism driving this migration is yet to be determined.

The Marajó Basin contributed to the drainage that fed the FOZ Basin during Equatorial Atlantic rifting (paleo–Tocantins River; Figs. 1, 6C, and 7C). At the time (130–103 Ma), the Marajó Basin was separated from the Parnaíba Basin located to the southeast by an arch preventing sediment transfer between the basins (e.g., Petri, 1987; Bajolet et al., 2022). During the Albian and onward (<110 Ma), this arch became subdued, allowing for the connection of the two basins (Bajolet et al., 2022). To account for the increase in accumulation in the FOZ Basin in the Late Cretaceous, we suggest that the watershed of the

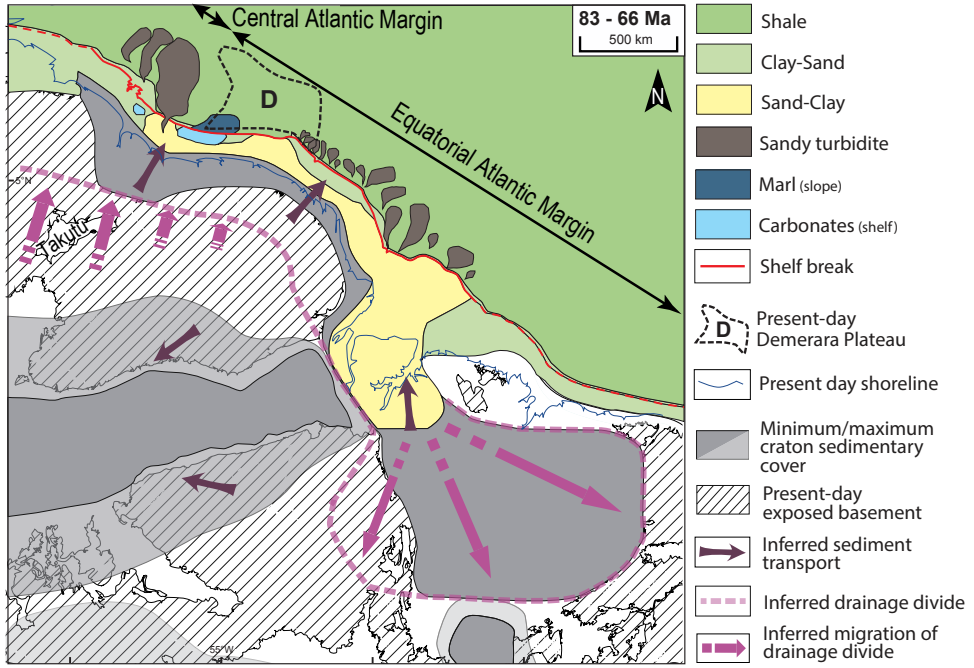

Figure 9. Inferred evolution of the drainage in the Late Cretaceous: southward growth of drainage to the Foz do Amazonas Basin and oceanward migration of the watershed of drainage to the Guiana-Suriname Basin. Drainage divides and sediment transport direction are from Bajolet et al. (2022).

drainage to the FOZ Basin migrated inland to incorporate the Parnaíba Basin area (Fig. 9).

In the Late Cretaceous (100–66 Ma), the drainage of the Guiana Shield was partitioning the sediment supply toward either inland cratonic basins or the rifted margin via northeastward-flowing coastal rivers (Bajolet et al., 2022; Figs. 6C–6E, 10, and 11D). We suggest that the watershed of this coastal drainage system migrated oceanward during that period, while the watershed of the coastal drainage to the FOZ Basin migrated inlandward (Fig. 9).

A Paleogene–Miocene Carbonate-Dominated Rifted Margin (66–6 Ma)

From 66 to 6 Ma, sediment supply to the margin was very reduced (Figs. 4F, 4G, and 5) and allowed for the growth of a major carbonate platform in the FOZ Basin (Figs. 7F and 7G). Subdued Paleogene–Miocene clastic fluxes to the margin were coeval with intense lateritic weathering over cratonic northern South America (Vasconcelos et al., 1994) and particularly on the Guiana Shield, which preserves extensive lateritic or bauxitic weathering mantles formed between 70 and 5 Ma (e.g., Théveniaut and Freyssinet, 2002).

Very low clastic fluxes along the Guiana Shield margin during the Paleogene and Miocene are in agreement with similarly subdued clastic flux estimates along the conjugated African Equatorial margin (Sierra Leone to Benin: Grimaud et al., 2018; Wildman et al., 2022). Clastic fluxes were subdued as well in basins of the Central Atlantic (Senegal: Lodhia et al., 2019) and of the South Atlantic rifted margins at that time (Niger: Grimaud et al., 2018; southern Africa: Baby et al., 2020; Pelotas Basin, offshore Brazil and Uruguay: Rohais et al., 2021). These peri-Atlantic low clastic fluxes are attributed to the Paleogene greenhouse climate and the mid-Miocene thermal optimum that favored sediment production and storage as regolith in forest-covered weathering profiles. During these periods, clastic sediment exports (i.e., regolith) to river systems were therefore reduced compared to solute exports produced by chemical weathering (e.g., Fairbridge and Finkl, 1980; Tardy and Roquin, 1998; Beauvais and Chardon, 2013; Grimaud et al., 2015). These periods were accordingly propitious to marine chemical sedimentation (e.g., carbonates, phosphates, attapulgite clay accumulation; Millot, 1970).

Plio-Quaternary Transcontinental Drainage (6–0 Ma)

After 6 Ma, the major increase in siliciclastic supply to the rifted margin basins records the establishment the modern Amazon River and Orinoco River courses linking the Andean retro-foreland basins to the Atlantic rifted margins (Hoorn et al., 2010; Figs. 3, 4H, and 5C). Clastic-dominated sedimentary systems were reinstalled along the whole margin (Fig. 7H). This includes

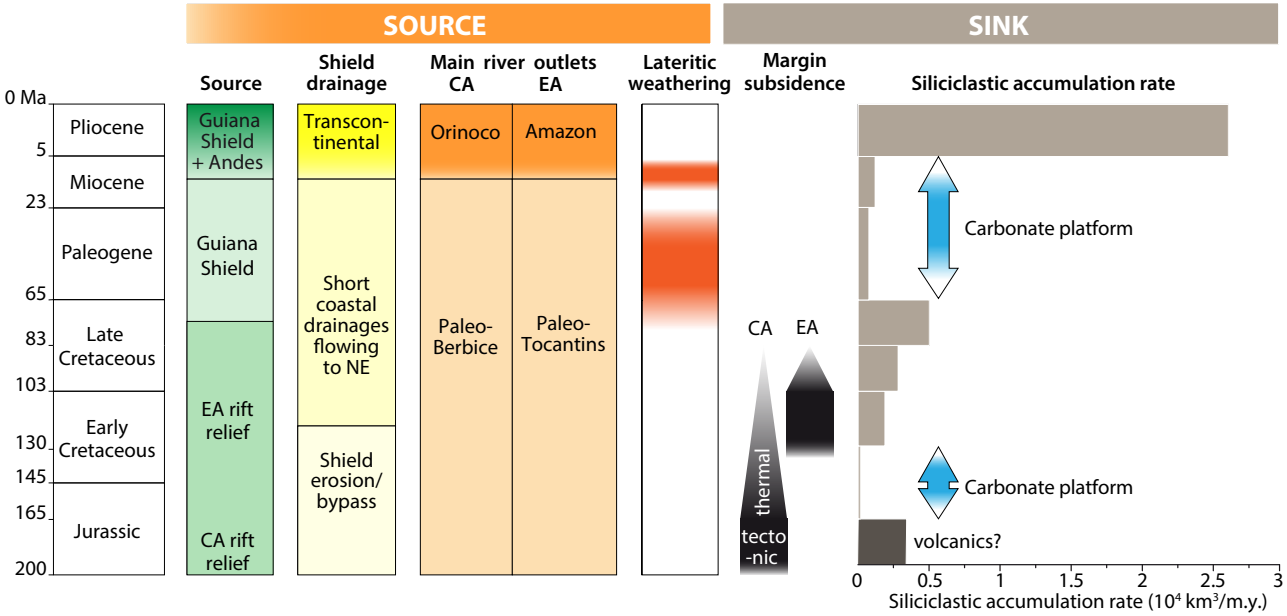

Figure 10. Synthesis of the sources-to-sink evolution of the Guyana Shield rifted margin. Main source of sediments and craton drainage are after Bajolet et al. (2022). Shades of colors indicate the progressive transition of the processes: green for the installation of the Andes domain as source, yellow for the installation of the transcontinental drainage, orange for the installation of the Orinoco and Amazon Rivers present day outlets, red for the intensity of weathering, black for the subsidence processes, and blue for the timing of carbonate deposition. Weathering intensity is after Vasconcelos et al. (1994). Main subsidence processes in the Guiana-Suriname and Foz do Amazonas Basins are after Loparev et al. (2021), and accumulation history after this study. EA—Equatorial Atlantic; CA—Central Atlantic. Note time scale is not linear.

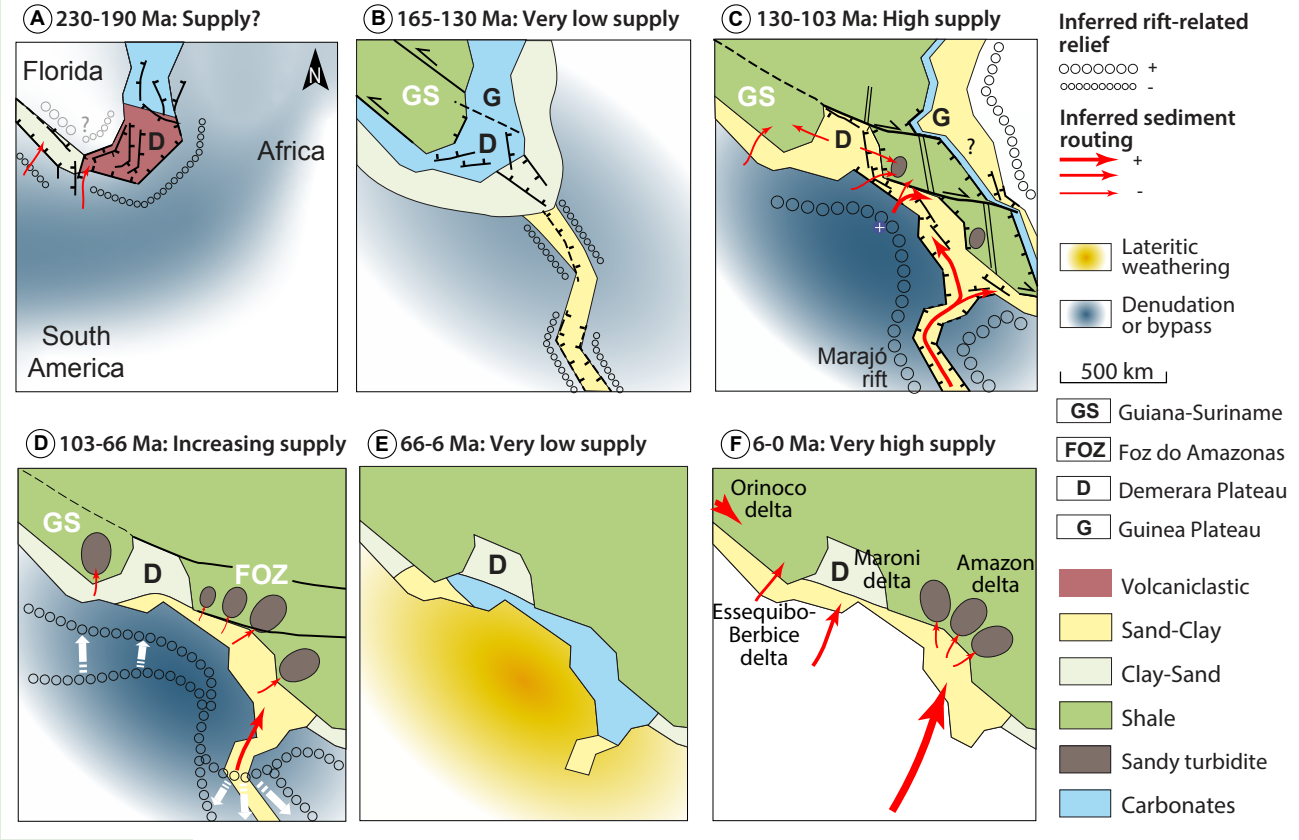

Figure 11. Schematic source-to-sink evolution of the Guiana Shield and Atlantic rifted margin. (A) 200–190 Ma: Central Atlantic rift with clastic deposits within the WNW-ESE rift segments, volcano-clastic deposits within NNE-SSW rift segment, and carbonate deposits along the north-south segment. (B) 165–130 Ma: Central Atlantic post-rift with the development of a carbonate platform along the whole margin and very low clastic supply. (C) 130–103 Ma: Central Atlantic post-rift and Equatorial Atlantic rift, break-up, and accretion with clastic deposits along both rifted margins and high clastic supply. (D) 103–66 Ma: Central and Equatorial Atlantic post-rift with clastic deposits along the margin, southward migration of the drainage divide resulting in an increasing accumulation in the Foz do Amazonas (FOZ) Basin, and oceanward migration of the divide of drainage to the Guiana-Suriname (GS) Basin resulting in decreasing accumulation in the GS Basin. (E) 66–6 Ma: Central and Equatorial Atlantic post-rift with intense weathering of the craton, development of a carbonate platform, and very low clastic supply. (F) 6–0 Ma: Central and Equatorial Atlantic post-rift with installation of the present-day routing of sediments and very high Andean clastic supply. Relative amplitude of inferred rift-related relief is indicated by pattern size and plus and minus signs. Relative sedimentary supply provided by the inferred sediment routing is indicated by arrow size and plus and minus signs. Divide locations are after Bajolet et al. (2022). Additional symbol explanation can be found in Figure 4.

the short coastal drainages such as the Maroni and Oyapok Rivers (Fig. 6H). Nonetheless, the main drainage systems feeding the rifted margin were the Essequibo-Berbice and Orinoco deltas in the GS Basin, the Maroni delta on the Demerara Plateau, and the Amazon delta in the FOZ Basin.

Source-to-Sink Integration

Overall, the accumulation history of the Guiana Shield rifted margin shows phases of very low siliciclastic supply (Figs. 11B and 11E) alternating with phases of higher siliciclastic supply (Figs. 10, 11C, and 11F). Periods of low siliciclastic input are associated with the development of carbonate platforms (Figs. 11B and 11E). They correspond to either (1) very limited relief variations in the drainage areas such as during the Late Jurassic for the GS Basin (Figs. 10 and 11B) or (2) periods of intense lateritic weathering of the cratonic source area such as in Paleogene–Miocene time for the FOZ Basin (Figs. 10 and 11E).

In contrast, periods of higher siliciclastic input to the Guiana Shield rifted margin basins correspond to either (1) relief-topographic growth in the drainage basin supplying the margin such as during the Equatorial Atlantic rifting in the Early Cretaceous (Figs. 10 and 11C), (2) drainage reorganization over a steadily eroding cratonic domain such as in the Late Cretaceous (Figs. 10 and 11D), or (3) tapping of sediments produced in the Andean orogenic domain such as during the Plio-Pleistocene via the present-day Orinoco and Amazon Rivers (Figs. 10 and 11F).

CONCLUSIONS

We determined the sedimentary budget of the Guiana Shield rifted margin from the stratigraphic architecture of the Guiana-Suriname, northern and

eastern Demerara, and Foz do Amazonas sedimentary basins. We investigated the implications of their histories of accumulation, depositional environments, and grain-size distribution in terms of sediment routing systems.

The accumulation history of the Guiana Shield rifted margin shows two phases of very low siliciclastic input associated with development of carbonate platforms. In the Late Cretaceous, reduced fluxes corresponded to a period of low continental relief variation following the rapid removal of the Central Atlantic rift-related relief. In the Neogene, low fluxes were due enhanced continental weathering that prevented solid exports from the Guiana Shield.

These periods alternated with phases of higher sediment supply to the rifted margin. In the Early Cretaceous, high clastic fluxes were due to the erosion of the Equatorial Atlantic rift-related relief that was steep enough to sustain a coarse siliciclastic supply to the margin for more than 40 m.y. In the Late Cretaceous, high clastic fluxes were due to changes in the organization of the drainage over the slowly eroding Guiana Shield: The drainage area of the Guiana-Suriname Basin decreased while the drainage area of the Foz do Amazonas Basin increased. In the Mio-Pliocene, the continental-scale reorganization of the drainage, establishing the present-day course of Orinoco and Amazon Rivers, massively increased the accumulation in the basins of the Guiana Shield rifted margin.

ACKNOWLEDGMENTS

We thank the Bureau de Recherches Géologiques et Minières and Total Energies for funding this work within the framework of the S2S project and the R&D Total Energies group for providing subsurface data. Subsurface data are under restrictive proprietary license and thus not open for distribution. We thank Cecile Robin for contributing to the accumulation calculation and Yann Montico for contributing to the isochore depth conversion. We also thank Nicholas Hayman for his review.

REFERENCES CITED

Allen, P.A., Armitage, J.J., Carter, A., Duller, R.A., Michael, N.A., Sinclair, H.D., Whitchurch, A.L., and Whittaker, A.C., 2013, The Q_s problem: Sediment volumetric balance of proximal foreland basin systems: Sedimentology, v. 60, p. 102–130, https://doi.org/10.1111/sed.12015.

Baby, G., Guillocheau, F., Braun, J., Robin, C., and Dall'Asta, M., 2020, Solid sedimentation rates history of the Southern African continental margins: Implications for the uplift history of the South African Plateau: Terra Nova, v. 32, p. 53–65, https://doi.org/10.1111/ter.12435.

Bajolet, F., Chardon, D., Rouby, D., Dall'Asta, M., Loparev, A., Couëffe, R., and Roig, J.-Y., 2022, The sediment routing systems of Northern South America since 250 Ma: Earth-Science Reviews, v. 232, https://doi.org/10.1016/j.earscirev.2022.104139.

Basile, C., Mascle, J., and Guiraud, R., 2005, Phanerozoic geological evolution of the Equatorial Atlantic domain: Journal of African Earth Sciences, v. 43, p. 275–282, https://doi.org/10.1016/j.jafrearsci.2005.07.011.

Basile, C., Maillard, A., Patriat, M., Gaullier, V., Loncke, L., Roest, W., Mercier de Lépinay, M., and Pattier, F., 2013, Structure and evolution of the Demerara Plateau, offshore French Guiana: Rifting, tectonic inversion and post-rift tilting at transform–divergent margins intersection: Tectonophysics, v. 591, p. 16–29, https://doi.org/10.1016/j.tecto.2012.01.010.

Basile, C., Girault, I., Paquette, J.-L., Agranier, A., Loncke, L., Heuret, A., and Poetisi, E., 2020, The Jurassic magmatism of the Demerara Plateau (offshore French Guiana) as a remnant of the Sierra Leone hotspot during the Atlantic rifting: Scientific Reports, v. 10, 7486, https://doi.org/10.1038/s41598-020-64333-5.

Beauvais, A., and Chardon, D., 2013, Modes, tempo, and spatial variability of Cenozoic cratonic denudation: The West African example: Geochemistry, Geophysics, Geosystems, v. 14, p. 1590–1608, https://doi.org/10.1002/ggge.20093.

Beauvais, A., Ruffet, G., Hénocque, O., and Colin, F., 2008, Chemical and physical erosion rhythms of the West African Cenozoic morphogenesis: The ^{39}Ar-^{40}Ar dating of supergene K-Mn oxides: Journal of Geophysical Research, v. 113, F04007, https://doi.org/10.1029/2008JF000996.

Benkhelil, J., Mascle, J., and Tricart, P., 1995, The Guinea continental margin: An example of a structurally complex transform margin: Tectonophysics, v. 248, p. 117–137, https://doi.org/10.1016/0040-1951(94)00246-6.

Beucher, R., and Huismans, R.S., 2020, Morphotectonic evolution of passive margins undergoing active surface processes: Large-scale experiments using numerical models: Geochemistry, Geophysics, Geosystems, v. 21, https://doi.org/10.1029/2019GC008884.

Brandão, J., and Feijó, F., 1994, Bacia da Foz do Amazonas: Boletim de Geociências da Petrobras, v. 8, p. 91–99.

Braun, J., 2018, A review of numerical modeling studies of passive margin escarpments leading to a new analytical expression for the rate of escarpment migration velocity: Gondwana Research, v. 53, p. 209–224, https://doi.org/10.1016/j.gr.2017.04.012.

Brune, S., Williams, S.E., Butterworth, N.P., and Müller, R.D., 2016, Abrupt plate accelerations shape rifted continental margins: Nature, v. 536, p. 201–204, https://doi.org/10.1038/nature18319.

Brune, S., Williams, S.E., and Müller, R.D., 2018, Oblique rifting: The rule, not the exception: Solid Earth, v. 9, p. 1187–1206, https://doi.org/10.5194/se-9-1187-2018.

Carozzi, A.V., 1981, Porosity models and oil exploration of Amapá carbonates, Paleogene, Foz do Amazonas Basin, offshore NW Brazil: Journal of Petroleum Geology, v. 4, p. 3–34, https://doi.org/10.1111/j.1747-5457.1981.tb00521.x.

Casson, M., Jeremiah, J., Calvès, G., de Ville de Goyet, F., Reuber, K., Bidgood, M., Reháková, D., Bulot, L., and Redfern, J., 2021, Evaluating the segmented post-rift stratigraphic architecture of the Guyanas continental margin: Petroleum Geoscience, v. 27, https://doi.org/10.1144/petgeo2020-099.

Chardon, D., Grimaud, J.-L., Rouby, D., Beauvais, A., and Christophoul, F., 2016, Stabilization of large drainage basins over geological time scales: Cenozoic West Africa, hot spot swell growth, and the Niger River: Geochemistry, Geophysics, Geosystems, v. 17, p. 1164–1181, https://doi.org/10.1002/2015GC006169.

Clift, P.D., and VanLaningham, S., 2010, A climatic trigger for a major Oligo-Miocene unconformity in the Himalayan foreland basin: Tectonics, v. 29, TC5014, https://doi.org/10.1029/2010TC002711.

Cordani, U.G., Ramos, V.A., Fraga, L.M., Cegarra, M., Delgado, I., de Souza, K.G., Gomes, F.E.M., and Schobbenhaus, C., 2016, Tectonic map of South America (2nd edition): Paris, Commission for the Geological Map of the World (CGMW)–Geological Survey of Brazil (CPRM)–Geological and Mining Survey of Argentina (SEGEMAR), scale 1:5,000,000.

Crawford, F.D., Szelewski, C.E., and Alvey, G.D., 1985, Geology and exploration in the Takutu graben of Guyana Brazil: Journal of Petroleum Geology, v. 8, p. 5–36, https://doi.org/10.1111/j.1747-5457.1985.tb00189.x.

Derycke, A., Gautheron, C., Barbarand, J., Bourbon, P., Aertgeerts, G., Simon-Labric, T., Sarda, P., Pinna-Jamme, R., Boukari, C., and Haurine, F., 2021, French Guiana margin evolution: From Gondwana break-up to Atlantic opening: Terra Nova, v. 33, p. 415–422, https://doi.org/10.1111/ter.12526.

DiPietro, J.A., 2013, Keys to the interpretation of geological history, *in* Landscape Evolution in the United States: An Introduction to the Geography, Geology, and Natural History: Waltham, Massachusetts, Elsevier, p. 327–344, https://doi.org/10.1016/B978-0-12-397799-1.00020-8.

Fairbridge, R.W., and Finkl, C.W., Jr., 1980, Cratonic erosional unconformities and peneplains: The Journal of Geology, v. 88, p. 69–86, https://doi.org/10.1086/628474.

Figueiredo, J.J.P., Zalán, P.V., and Soares, E.F., 2007, Bacia da Foz do Amazonas: Boletim de Geociências da Petrobras, v. 15, p. 299–309.

Gillard, M., Sauter, D., Tugend, J., Tomasi, S., Epin, M.-E., and Manatschal, G., 2017, Birth of an oceanic spreading center at a magma-poor rift system: Scientific Reports, v. 7, 15072, https://doi.org/10.1038/s41598-017-15522-2.

Grimaud, J.-L., Chardon, D., and Beauvais, A., 2014, Very long-term incision dynamics of big rivers: Earth and Planetary Science Letters, v. 405, p. 74–84, https://doi.org/10.1016/j.epsl.2014.08.021.

Grimaud, J.-L., Chardon, D., Metelka, V., Beauvais, A., and Bamba, O., 2015, Neogene cratonic erosion fluxes and landform evolution processes from regional regolith mapping (Burkina

Faso, West Africa): Geomorphology, v. 241, p. 315–330, https://doi.org/10.1016/j.geomorph.2015.04.006.
Grimaud, J.-L., Rouby, D., Chardon, D., and Beauvais, A., 2018, Cenozoic sediment budget of West Africa and the Niger delta: Basin Research, v. 30, p. 169–186, https://doi.org/10.1111/bre.12248.
Guillocheau, F., Rouby, D., Robin, C., Helm, C., Rolland, N., Le Carlier de Veslud, C., and Braun, J., 2012, Quantification and causes of the terrigeneous sediment budget at the scale of a continental margin: A new method applied to the Namibia-South Africa margin: Basin Research, v. 24, p. 3–30, https://doi.org/10.1111/j.1365-2117.2011.00511.x.
Guiraud, R., Binks, R.M., Fairhead, J.D., and Wilson, M., 1992, Chronology and geodynamic setting of Cretaceous-Cenozoic rifting in West and Central Africa: Tectonophysics, v. 213, p. 227–234, https://doi.org/10.1016/0040-1951(92)90260-D.
Heine, C., Zoethout, J., and Müller, R.D., 2013, Kinematics of the South Atlantic rift: Solid Earth, v. 5, p. 41–116, https://doi.org/10.5194/sed-5-41-2013.
Hoorn, C., Guerrero, J., Sarmiento, G.A., and Lorente, M.A., 1995, Andean tectonics as a cause for changing drainage patterns in Miocene northern South America: Geology, v. 23, p. 237–240, https://doi.org/10.1130/0091-7613(1995)023<0237:ATAACF>2.3.CO;2.
Hoorn, C., Wesselingh, F.P., ter Steege, H., Bermudez, M.A., Mora, A., Sevink, J., Sanmartín, I., Sanchez-Meseguer, A., Anderson, C.L., Figueiredo, J.P., Jaramillo, C., Riff, D., Negri, F.R., Hooghiemstra, H., Lundberg, J., Stadler, T., Särkinen, T., and Antonelli, A., 2010, Amazonia through time: Andean uplift, climate change, landscape evolution, and biodiversity: Science, v. 330, p. 927–931, https://doi.org/10.1126/science.1194585.
Hoorn, C., Bogotá-A, G.R., Romero-Baez, M., Lammertsma, E.I., Flantua, S.G.A., Dantas, E.L., Dino, R., do Carmo, D.A., and Chemale, F., Jr., 2017, The Amazon at sea: Onset and stages of the Amazon River from a marine record, with special reference to Neogene plant turnover in the drainage basin: Global and Planetary Change, v. 153, p. 51–65, https://doi.org/10.1016/j.gloplacha.2017.02.005.
Klitgord, K.D., and Schouten, H., 1986, Plate kinematics of the central Atlantic., *in* Vogt P.R., and Tucholke, B.E., eds., The Western North Atlantic Region: Boulder, Colorado, Geological Society of America, The Geology of North America, v. M, p. 351–378, https://doi.org/10.1130/DNAG-GNA-M.351.
Lodhia, B.H., Roberts, G.G., Fraser, A.J., Jarvis, J., Newton, R., and Cowan, R.J., 2019, Observation and simulation of solid sedimentary flux: Examples from northwest Africa: Geochemistry, Geophysics, Geosystems, v. 20, p. 4613–4634, https://doi.org/10.1029/2019GC008262.
Loncke, L., Roest, W.R., Klingelhoefer, F., Basile, C., Graindorge, D., Heuret, A., Marcaillou, B., Museur, T., Fanget, A.S., and Mercier de Lépinay, M., 2020, Transform marginal plateaus: Earth-Science Reviews, v. 203, https://doi.org/10.1016/j.earscirev.2019.102940.
Loparev, A., Rouby, D., Chardon, D., Dall'Asta, M., Sapin, F., Bajolet, F., Ye, J., and Paquet, F., 2021, Superimposed rifting at the junction of the Central and Equatorial Atlantic: Formation of the passive margin of the Guiana Shield: Tectonics, v. 40, https://doi.org/10.1029/2020TC006159.
Maffre, P., Ladant, J.-B., Moquet, J.-S., Carretier, S., Labat, D., and Goddéris, Y., 2018, Mountain ranges, climate and weathering. Do orogens strengthen or weaken the silicate weathering carbon sink?: Earth and Planetary Science Letters, v. 493, p. 174–185, https://doi.org/10.1016/j.epsl.2018.04.034.
Martinsen, O.J., Sømme, T.O., Thurmond, J.B., Helland-Hansen, W., and Lunt, I., 2010, Source-to-sink systems on passive margins: Theory and practice with an example from the Norwegian continental margin, *in* Vining, B.A., and Pickering, S.C., eds., Petroleum Geology: From Mature Basins to New Frontiers—Proceedings of the 7th Petroleum Geology Conference: Geological Society of London Petroleum Geology Conference Series 7, p. 913–920, https://doi.org/10.1144/0070913.
Mascle, J., Blarez, E., and Marinho, M., 1988, The shallow structures of the Guinea and Ivory Coast–Ghana transform margins: Their bearing on the Equatorial Atlantic Mesozoic evolution: Tectonophysics, v. 155, p. 193–209, https://doi.org/10.1016/0040-1951(88)90266-1.
McConnell, R.B., 1969, Fundamental fault zones in the Guiana and West African shields in relation to presumed axes of Atlantic spreading: Geological Society of America Bulletin, v. 80, p. 1775–1782, https://doi.org/10.1130/0016-7606(1969)80[1775:NADFFZ]2.0.CO;2.
Mercier de Lépinay, M., 2016, Inventaire mondial des marges transformantes et évolution tectono-sédimentaire des plateaux de Demerara et de Guinée [Ph.D. thesis]: Perpignan, France, Université de Perpignan, 334 p.
Métivier, F., and Gaudemer, Y., 1999, Stability of output fluxes of large rivers in South and East Asia during the last 2 million years: Implications on floodplain processes: Basin Research, v. 11, p. 293–303, https://doi.org/10.1046/j.1365-2117.1999.00101.x.
Milliman, J.D., and Farnsworth, K.L., 2013, River Discharge to the Coastal Ocean: A Global Synthesis: Cambridge, UK, Cambridge University Press, 390 p.
Millot, G., 1970, Geology of Clays: Berlin, Springer-Verlag, 429 p., https://doi.org/10.1007/978-3-662-41609-9.
Moulin, M., Aslanian, D., and Unternehr, P., 2010, A new starting point for the South and Equatorial Atlantic Ocean: Earth-Science Reviews, v. 98, p. 1–37, https://doi.org/10.1016/j.earscirev.2009.08.001.
Museur, T., Graindorge, D., Klingelhoefer, F., Roest, W.R., Basile, C., Loncke, L., and Sapin, F., 2021, Deep structure of the Demerara Plateau: From a volcanic margin to a Transform Marginal Plateau: Tectonophysics, v. 803, https://doi.org/10.1016/j.tecto.2020.228645.
Nemčok, M., Rybár, S., Odegard, M., Dickson, W., Pelech, O., Ledvényiová, L., Matejová, M., Molčan, M., Hermeston, S., Jones, D., Cuervo, E., Cheng, R., and Forero, G., 2016, Development history of the southern terminus of the Central Atlantic: Guyana–Suriname case study, *in* Nemčok, M., Rybár, S., Sinha, S.T., Hermeston, S.A., and Ledvényiová, L., eds., Transform Margins: Development, Controls and Petroleum Systems: Geological Society, London, Special Publication 431, p. 145–178, https://doi.org/10.1144/SP431.10.
NOAA National Geophysical Data Center, 2009, ETOPO1 1 arc-minute global relief model: NOAA National Centers for Environmental Information, https://doi.org/10.7289/V5C8276M (last accessed February 2019).
Petri, S., 1987, Cretaceous paleogeographic maps of Brazil: Palaeogeography, Palaeoclimatology, Palaeoecology, v. 59, p. 117–168, https://doi.org/10.1016/0031-0182(87)90077-0.
Pindell, J.L., 1985, Alleghenian reconstruction and subsequent evolution of the Gulf of Mexico, Bahamas, and Proto-Caribbean: Tectonics, v. 4, p. 1–39, https://doi.org/10.1029/TC004i001p00001.
Pindell, J.L., and Kennan, L., 2009, Tectonic evolution of the Gulf of Mexico, Caribbean and northern South America in the mantle reference frame: An update, *in* James, K.H., Lorente, M.A., and Pindell, J.L., eds., The Origin and Evolution of the Caribbean Plate: Geological Society, London, Special Publication 328, p. 1–55, https://doi.org/10.1144/SP328.1.
Ramos, V.A., 1999, Plate tectonic setting of the Andean Cordillera: Episodes, v. 22, p. 183–190, https://doi.org/10.18814/epiiugs/1999/v22i3/005.
Reuber, K.R., Pindell, J., and Horn, B.W., 2016, Demerara Rise, offshore Suriname: Magma-rich segment of the Central Atlantic Ocean, and conjugate to the Bahamas hot spot: Interpretation (Tulsa), v. 4, p. T141–T155, https://doi.org/10.1190/INT-2014-0246.1.
Roddaz, M., Dera, G., Mourlot, Y., Calvès, G., Kim, J.-H., Chaboureau, A.-C., Mounic, S., and Raisson, F., 2021, Provenance constraints on the Cretaceous-Paleocene erosional history of the Guiana Shield as determined from the geochemistry of clay-size fraction of sediments from the Arapaima-1 well (Guyana-Suriname basin): Marine Geology, v. 434, https://doi.org/10.1016/j.margeo.2021.106433.
Rohais, S., Lovecchio, J.P., Abreu, V., Miguez, M., and Paulin, S., 2021, High-resolution sedimentary budget quantification—Example from the Cenozoic deposits in the Pelotas Basin, South Atlantic: Basin Research, v. 33, p. 2252–2280, https://doi.org/10.1111/bre.12556.
Rouby, D., Bonnet, S., Guillocheau, F., Gallagher, K., Robin, C., Biancotto, F., Dauteuil, O., and Braun, J., 2009, Sediment supply to the Orange sedimentary system over the last 150 My: An evaluation from sedimentation/denudation balance: Marine and Petroleum Geology, v. 26, p. 782–794, https://doi.org/10.1016/j.marpetgeo.2008.08.004.
Rouby, D., Braun, J., Robin, C., Dauteuil, O., and Deschamps, F., 2013, Long-term stratigraphic evolution of Atlantic-type passive margins: A numerical approach of interactions between surface processes, flexural isostasy and 3D thermal subsidence: Tectonophysics, v. 604, p. 83–103, https://doi.org/10.1016/j.tecto.2013.02.003.
Sapin, F., Davaux, M., Dall'asta, M., Lahmi, M., Baudot, G., and Ringenbach, J.-C., 2016, Post-rift subsidence of the French Guiana hyper-oblique margin: From rift-inherited subsidence to Amazon deposition effect, *in* Nemčok, M., Rybár, S., Sinha, S.T., Hermeston, S.A., and Ledvényiová, L., eds., Transform Margins: Development, Controls and Petroleum Systems: Geological Society, London, Special Publication 431, p. 125–144, https://doi.org/10.1144/SP431.11.
Schettino, A., and Turco, E., 2009, Breakup of Pangaea and plate kinematics of the central Atlantic and Atlas regions: Geophysical Journal International, v. 178, p. 1078–1097, https://doi.org/10.1111/j.1365-246X.2009.04186.x.
Shephard, G.E., Müller, R.D., Liu, L., and Gurnis, M., 2010, Miocene drainage reversal of the Amazon River driven by plate-mantle interaction: Nature Geoscience, v. 3, p. 870–875, https://doi.org/10.1038/ngeo1017.
Svartman Dias, A.E., Lavier, L.L., and Hayman, N.W., 2015, Conjugate rifted margins width and asymmetry: The interplay between lithospheric strength and thermomechanical processes:

Journal of Geophysical Research: Solid Earth, v. 120, p. 8672–8700, https://doi.org/10.1002/2015JB012074.

Tardy, Y., and Roquin, C., 1998, Dérive des continents, paléoclimats et altérations tropicales: Orléans, France, Editions BRGM, 473 p.

Theunissen, T., and Huismans, R.S., 2019, Long-term coupling and feedback between tectonics and surface processes during non-volcanic rifted margin formation: Journal of Geophysical Research: Solid Earth, v. 124, p. 12,323–12,347, https://doi.org/10.1029/2018JB017235.

Théveniaut, H., and Freyssinet, P., 2002, Timing of lateritization on the Guiana Shield: Synthesis of paleomagnetic results from French Guiana and Suriname: Palaeogeography, Palaeoclimatology, Palaeoecology, v. 178, p. 91–117, https://doi.org/10.1016/S0031-0182(01)00404-7.

Torsvik, T.H., and Cocks, L.R.M., 2013, Gondwana from top to base in space and time: Gondwana Research, v. 24, p. 999–1030, https://doi.org/10.1016/j.gr.2013.06.012.

Trude, J., Kilsdonk, B., Grow, T., and Ott, B., 2022, The structure and tectonics of the Guyana Basin, *in* Nemčok, M., Doran, H., Doré, A.G., Ledvényiová, L., and Rybár, S., eds., Tectonic Development, Thermal History and Hydrocarbon Habitat Models of Transform Margins: their Differences from Rifted Margins: Geological Society, London, Special Publication 524, https://doi.org/10.1144/SP524-2021-117.

van Soelen, E.E., Kim, J.-H., Santos, R.V., Dantas, E.L., Vasconcelos de Almeida, F., Pires, J.P., Roddaz, M., and Sinninghe Damsté, J.S., 2017, A 30 Ma history of the Amazon River inferred from terrigenous sediments and organic matter on the Ceará Rise: Earth and Planetary Science Letters, v. 474, p. 40–48, https://doi.org/10.1016/j.epsl.2017.06.025.

Vasconcelos, P.M., Renne, P.R., Brimhall, G.H., and Becker, T.A., 1994, Direct dating of weathering phenomena by $^{40}Ar/^{39}Ar$ and K-Ar analysis of supergene K-Mn oxides: Geochimica et Cosmochimica Acta, v. 58, p. 1635–1665, https://doi.org/10.1016/0016-7037(94)90565-7.

Watts, A.B., Rodger, M., Peirce, C., Greenroyd, C.J., and Hobbs, R.W., 2009, Seismic structure, gravity anomalies, and flexure of the Amazon continental margin, NE Brazil: Journal of Geophysical Research, v. 114, B07103, https://doi.org/10.1029/2008JB006259.

Whittaker, A.C., Duller, R.A., Springett, J., Smithells, R.A., Whitchurch, A.L., and Allen, P.A., 2011, Decoding downstream trends in stratigraphic grain size as a function of tectonic subsidence and sediment supply: Geological Society of America Bulletin, v. 123, p. 1363–1382, https://doi.org/10.1130/B30351.1.

Wildman, M., Webster, D., Brown, R., Chardon, D., Rouby, D., Ye, J., Huyghe, D., and Dall'Asta, M., 2019, Long-term evolution of the West African transform margin: Estimates of denudation from Benin using apatite thermochronology: Journal of the Geological Society, v. 176, p. 97–114, https://doi.org/10.1144/jgs2018-078.

Wildman, M., Brown, R., Ye, J., Chardon, D., Rouby, D., Kouamelan, A.N., and Dall'Asta, M., 2022, Contrasting thermal evolution of the West African Equatorial and Central Atlantic continental margins: Gondwana Research, v. 111, p. 249–264, https://doi.org/10.1016/j.gr.2022.08.010.

Wolf, L., Huismans, R.S., Rouby, D., Gawthorpe, R.L., and Wolf, S.G., 2022, Links between faulting, topography, and sediment production during continental rifting: Insights from coupled surface process, thermomechanical modeling: Journal of Geophysical Research: Solid Earth, v. 127, https://doi.org/10.1029/2021JB023490.

Yang, W.X., and Escalona, A., 2011, Tectonostratigraphic evolution of the Guyana Basin: American Association of Petroleum Geologists Bulletin, v. 95, p. 1339–1368, https://doi.org/10.1306/01031110106.

Ye, J., Chardon, D., Rouby, D., Guillocheau, F., Dall'asta, M., Ferry, J.-N., and Broucke, O., 2017, Paleogeographic and structural evolution of northwestern Africa and its Atlantic margins since the early Mesozoic: Geosphere, v. 13, p. 1254–1284, https://doi.org/10.1130/GES01426.1.

Ye, J., Rouby, D., Chardon, D., Dall'asta, M., Guillocheau, F., Robin, C., and Ferry, J.N., 2019, Post-rift stratigraphic architectures along the African margin of the Equatorial Atlantic: Part I The influence of extension obliquity: Tectonophysics, v. 753, p. 49–62, https://doi.org/10.1016/j.tecto.2019.01.003.

Zalán, P.V., and Matsuda, N.S., 2007, Bacia do Marajó: Boletim de Geociências da Petrobras, v. 15, p. 311–319.